JOURNAL OF VIRAL HEPATITIS
JVH

Journal of Viral Hepatitis, 2011, **18**, 206–215 doi:10.1111/j.1365-2893.2010.01301.x

Four-year study of lamivudine and adefovir combination therapy in lamivudine-resistant hepatitis B patients: influence of hepatitis B virus genotype and resistance mutation pattern

J. Inoue, Y. Ueno, Y. Wakui, H. Niitsuma, K. Fukushima, Y. Yamagiwa, M. Shiina, Y. Kondo, E. Kakazu, K. Tamai, N. Obara, T. Iwasaki and T. Shimosegawa *Division of Gastroenterology, Tohoku University Graduate School of Medicine, Aoba-ku, Sendai, Japan*

Received September 2009; accepted for publication January 2010

SUMMARY. To investigate the efficacy of long-term lamivudine (3TC) and adefovir dipivoxil (ADV) combination therapy in 3TC-resistant chronic hepatitis B virus (HBV) infected patients, we analysed 28 3TC-resistant patients treated with the combination therapy during 47 months (range, 9–75). At 12, 24, 36, and 48 months, the rates of virological response with undetectable HBV DNA (≤2.6 log copies/mL) were 56, 80, 86, and 92%, respectively. Among 17 hepatitis B e antigen (HBeAg)-positive patients, HBeAg disappeared in 24% at 12 months, 25% at 24 months, 62% at 36 months, and 88% at 48 months. When HBV genotypes were compared, patients with genotype B achieved virological response significantly more rapidly than those with genotype C ($P = 0.0496$). One patient developed virological breakthrough after 54 months, and sequence analysis of HBV obtained from the patient was performed. An rtA200V mutation was present in the majority of HBV clones, in addition to the 3TC-resistant mutations of rtL180M+M204V. The rtN236T ADV-resistant mutation was observed in only 25% clones. *In vitro* analysis showed that the rtA200V mutation recovered the impaired replication capacity of the clone with the rtL180M+M204V mutations and induced resistance to ADV. Moreover, rtT184S and rtS202C, which are known entecavir-resistant mutations, emerged in some rtL180M+M204V clones without rtA200V or rtN236T. In conclusion, 3TC+ADV combination therapy was effective for most 3TC-resistant patients, especially with genotype B HBV, but the risk of emergence of multiple drug-resistant strains with long-term therapy should be considered. The mutation rtA200V with rtL180M+M204V may be sufficient for failure of 3TC+ADV therapy.

Keywords: chronic hepatitis B, drug resistance, HBV, rtA200V.

INTRODUCTION

Hepatitis B virus (HBV) causes acute and chronic infection, and chronic hepatitis often leads to liver cirrhosis and hepatocellular carcinoma (HCC) [1]. HBV contains a small (3.2 kb), circular, partially double-stranded DNA genome, and nucleoside or nucleotide analogues inhibit HBV replication by interfering with reverse transcriptase/DNA polymerase of the virus [2]. Although therapy with these drugs results in virological, biochemical, and histological improvement in most patients [3], the effect is often transient because of the emergence of drug-resistant HBV mutants [4].

Lamivudine (3TC), a nucleoside analogue of L-deoxycytidine, is associated with highly frequent emergence of drug-resistant mutants: the cumulative rate is about 20% per year [5,6]. Mutations that result in the replacement of methionine at amino acid 204 to valine or isoleucine (rtM204V/I) within the tyrosine-methionine-aspartate-aspartate (YMDD) motif in the reverse transcriptase (RT) region of HBV polymerase are found in most of the 3TC-resistant isolates [7]. Compensatory mutations rtV173L and rtL180M, which restore the replication capacity of the YMDD mutant *in vitro*, are observed frequently together with the YMDD mutation [8,9]. Adefovir dipivoxil (ADV) is a phosphonate nucleotide analogue of adenosine monophosphate, and ADV-resistance rates are lower than those of 3TC [10]. Two mutations, rtA181V/T and rtN236T, are associated with resistance to ADV [11–14], and the cumulative 5-year occurrence of genotypic resistance is reported to be 29% [15]. *In vitro* studies showed that these mutations confer a weaker

Abbreviations: ADV, adefovir dipivoxil; ALT, alanine aminotransferase; eGFR, estimated glomerular filtration rate; ETV, entecavir; HBeAg, hepatitis B e antigen; HBsAg, hepatitis B surface antigen; HBV, hepatitis B virus; HCC, hepatocellular carcinoma; PCR, polymerase chain reaction; RT, reverse transcriptase; TDF, tenofovir disoproxil fumarate.

Correspondence: Yoshiyuki Ueno, Division of Gastroenterology, Tohoku University Graduate School of Medicine, 1-1 Seiryo, Aoba-ku, Sendai 980-8574, Japan. E-mail: yueno@mail.tains.tohoku.ac.jp

decrease in the susceptibility to ADV, in comparison with the greater decrease in 3TC susceptibility because of the YMDD mutant [11,16]. This finding may explain the lower rate of the emergence of ADV resistance.

Although the number of approved drugs has increased in recent years, the treatment of chronic HBV infection remains a clinical challenge. Especially, how to manage drug-resistant patients including 3TC-resistant patients is a major problem. Continuation of 3TC monotherapy or retreatment with 3TC after its temporary discontinuation is ineffective options for 3TC-resistant patients [17]: the lack of any further benefit and the possibility of rapid re-emergence of resistant HBV have been reported [18]. Against 3TC-resistant HBV, ADV and entecavir (ETV) have a suppressive effect *in vivo* and *in vitro* [19–21]. Combination therapy of ADV and 3TC is effective for 3TC-refractory patients and has a low frequency of viral breakthrough [22]: the 3-year cumulative rate of *de novo* resistant mutants was 4% with no development of viral breakthrough in 3TC-resistant patients. However, further longer-term efficacy of the combination therapy remains unknown. ETV is a potent drug with infrequent development of resistance for treatment-naïve patients [23]. ETV monotherapy was shown to be effective during the first year of therapy in 3TC-resistant patients [20], but pre-existing 3TC-resistant mutants are favourable for the emergence of ETV resistance [21], and a comparatively high rate of the emergence of ETV-resistant strains has been reported in long-term studies [23]. Therefore, ETV monotherapy seems to be a less attractive option for the long-term treatment of 3TC-resistant patients.

Several previous reports have described the differences in the responses to antiviral therapy between HBV genotypes. A case–control study of 3TC treatment for genotypes B and C showed that the responses were not different, but the emergence of the YMDD mutation was more frequent in genotype C [24]. It was also reported that the YMDD mutation and breakthrough hepatitis developed more often in patients with genotype A than in patients with genotype B or C [25]. However, the impact of the genotype on the efficacy to ADV is uncertain.

Here, we studied the long-term efficacy of 28 3TC-resistant patients treated with the combination of 3TC and ADV and compared the response between HBV genotypes. Sequence analysis of HBV from a patient with resistance to the combination therapy was performed, and *in vitro* drug susceptibility of the mutant HBV clones was assessed to clarify the mechanism of the emergence of resistance.

MATERIALS AND METHODS

Patients

A total of 28 consecutive Japanese patients with chronic HBV infection who were treated with 3TC+ADV at Tohoku University Hospital from June 2003 to August 2009 for more than 6 months were enrolled in this study. All patients developed virological breakthrough during 3TC monotherapy, and ADV was added in. Virological breakthrough was defined as an increase in the serum HBV DNA level of ≥1 log copies/mL, which was determined using the Amplicor HBV monitor test (Roche Diagnostics, Tokyo, Japan), at two or more consecutive examinations in comparison with the lowest level after treatment. To evaluate renal function, the estimated glomerular filtration rate (eGFR) level using the Cockcroft-Gault formula [(140 - age) × (weight in kilograms) × (0.85 if female)/(72 × serum creatinine)] [26] was calculated. No patients were infected with HCV, nor had a history of other liver diseases. The patients were evaluated for the rate of virological response (undetectable HBV DNA: <2.6 log copies/mL), biochemical response [alanine aminotransferase (ALT) normalization: ≤35 IU/L], hepatitis B e antigen (HBeAg) loss, and virological breakthrough.

Antiviral treatment

Adefovir dipivoxil was administered at a dosage of 10 mg/day in all but one patient in addition to 3TC at a dosage of 100 mg/day. One patient received 10 mg of ADV on alternate days and 50 mg/day of 3TC daily because of reduced eGFR at the start of treatment. This occurred when the eGFR level dropped to <50 mL/min.

Determination of HBV genotype

The HBV genotype was determined as described previously [27] with minor modifications. Briefly, total DNA was extracted from 50 μL of serum sample by QIAamp Blood Mini kit (QIAGEN GmbH, Hilden, Germany) and subjected to nested polymerase chain reaction (PCR) with high fidelity polymerase (PrimeSTAR HS DNA polymerase; TaKaRa Bio Inc., Shiga, Japan), to amplify a 396-nt sequence in the S gene. The amplification products were sequenced on both strands directly using the BigDye Terminator v3.1 Cycle Sequencing kit on an ABI PRISM 3100 Genetic Analyzer (Applied Biosystems, Foster City, CA, USA). Sequence analysis was performed using Genetyx-Mac (Version 12.2.7; Genetyx Corp., Tokyo, Japan). The genotype of HBV was determined by phylogenetic analysis with HBV isolates whose genotype was known.

Sequencing analysis of HBV reverse transcriptase region

Total DNA extracted from 50 μL of serum sample was subjected to nested PCR to amplify the 1148-nt sequence [nt 52 to 1199, the nucleotide numbers are in accordance with a genotype C HBV isolate of 3,215 nt (AB033550)] including the RT region of HBV polymerase. The first-round PCR was carried out with primers B026 [5′-TCA TCC WCA GGC CAT GCA GTG GA-3′ (W = A or T)] and B025 (5′-CTA GGA GTT CCG CAG TAT GGA TCG-3′), and the second round with

primers B011 [5′-YTT YCC TGC TGG TGG CTC CAG TTC-3′ (Y = C or T)] and B024 (5′-GGG GTT GCG TCA GCA AAC ACT TG-3′). The amplification products were sequenced on both strands directly or after cloning into pUC118. Sequencing analysis after cloning was performed at nt 497-1161.

Construction of plasmid

A cloned mutant sequence including the RT region from a sample obtained after the development of 3TC and ADV resistance was digested with BlnI (TaKaRa Bio Inc.) and EcoT22I (TaKaRa Bio Inc.). The digested fragment (nt 179-1068) was ligated into the BlnI-EcoT22I site of pBFH2R, which contained a 1.3-fold HBV genome [28]. Quick Change II-E Site-Directed Mutagenesis kit (Stratagene, La Jolla, CA, USA) was used to introduce nucleotide substitutions into the plasmid. Each mutation found in the RT region, rtL180M [C to A at nt 667 (C667A)], rtT184S (A679T), rtA200V (C728T), rtS202C (A733T), rtM204V (A739G), and rtN236T (A836C), was converted into the wild type or another mutant nucleotide. To construct plasmids with combined nucleotide substitutions, these converted plasmids were used next as templates. As a result, variant constructs harbouring rtM204I, rtL180M+M204V, rtL180M+T184S+M204V, rtL180M+A200V+M204V, rtL180M+S202C+M204V, rtL180M+M204V+N236T, and rtL180M+A200V+M204V+N236T were composed, and all constructs were sequenced to confirm the nucleotide substitutions.

Cell culture and transfection

Human hepatoma HepG2 cells were cultured in Dulbecco's modified Eagle medium supplemented with 10% bovine serum at 37 °C and 5% CO_2. Cells were seeded in 24-well plates at 1.25×10^5 cells/well. On the next day, 375 ng of plasmid DNA were transfected into these cells using TransIT LT-1 Transfection Reagent (Mirus, Madison, WI, USA), and cells were washed twice with phosphate-buffered saline after 4 h. Five hundred microliter of the medium and various amounts of adefovir (Toronto Research Chemicals Inc., Ontario, Canada) were added, and the culture supernatant was collected 4 days later. Experiments were performed at least in triplicate.

Real-time PCR and determination of IC_{50}

HBV DNA in the culture supernatant was quantified by real-time PCR as described previously [28] to determine the 50% inhibitory concentration (IC50) for ADV of each mutant HBV clone. Briefly, to digest the input plasmid DNA in the culture supernatant, 5 μL of the supernatant were treated with 5 units of DNase I (TaKaRa Bio Inc.) at 37 °C for 2 h, and the reaction was stopped with EDTA. Then, total DNA was extracted with a QIAamp DNA Blood Mini kit, and 10 μL of 200 μL DNA solution were subjected to real-time PCR using a LightCycler (Roche Diagnostics). Dose–response curves were plotted to determine the ADV IC50.

Statistical analysis

Statistical analyses were performed using Fisher's exact probability test for comparison of proportions between two groups and Mann–Whitney *U* test for comparison of continuous variables between two groups. The cumulative rate of undetectable HBV DNA or ALT normalization was calculated using the Kaplan–Meier method, and differences between the curves were tested using Log-rank test. Differences were considered to be statistically significant when $P < 0.05$.

RESULTS

Study profile

The demographic and clinical profiles of the 28 patients [20 men and 8 women, median age 53.5 years (range 18–72)] at commencement of 3TC+ADV therapy are shown in Table 1. One (3.6%), 7 (25.0%), and 19 (67.9%) patients had HBV of genotypes A, B, and C, respectively. Eight (28.6%) patients had cirrhosis, 7 (25.0%) had HCC, and 17 (60.7%) patients were HBeAg positive. The mutations of the YMDD motif were determined by direct sequencing, and the YIDD, YVDD, and YIDD+YVDD mixed pattern were found in 14 (50%), 11 (39%), and 2 (7%)of the patients, respectively. Only one (4%) patient had no mutation in the YMDD motif. There were no significant differences in the profiles between patients with genotype B and those with genotype C.

Response to lamivudine and adefovir dipivoxil combination therapy

The 3TC-resistant patients treated with the combination therapy were followed up for a median of 47 months (range, 9–75). All patients continued to be treated with 3TC and ADV until virological breakthrough. The 6-, 12-, 24-, 36-, and 48-month rates of virological response with HBV DNA ≤ 2.6 log copies/mL were 39, 56, 80, 86, and 92%, respectively (Table 2). The ALT normalization rates were 57% at 6 months, 70% at 12 months, 84% at 24 months, 82% at 36 months, and 77% at 48 months. When compared between genotype B and C, the results of patients with genotype B tended to be favourable for both virological and biochemical response (Figs 1a,b). The cumulative probability of undetectable HBV DNA was significantly higher in genotype B than in genotype C ($P = 0.0496$), whereas there was no significant difference in that of ALT normalization. Notably, patients with genotype B achieved early virological response (HBV DNA < 2.6 log copies/mL at 6 months) significantly more frequently than those with genotype C

Table 1 Demographic and clinical characteristics of the 28 lamivudine-resistant patients at the start of adefovir addition to the treatment

	Overall (n = 28)*	Genotype B (n = 7)	Genotype C (n = 20)
Age (years), median (range)	53.5 (18–72)	51.0 (18–72)	53.5 (35–68)
Male patients, no. (%)	20 (71.4)	5 (71.4)	14 (70.0)
Patients with cirrhosis, no. (%)	8 (28.6)	1 (14.3)	7 (35.0)
Patients with HCC, no. (%)	7 (25.0)	0 (0)	7 (35.0)
HBeAg positive, no. (%)	17 (60.7)	3 (42.9)	13 (65.0)
HBV DNA (log copies/mL), median (range)	7.6 (4.3 to >7.6)	7.2 (5.3 to >7.6)	7.6 (4.3 to >7.6)
Patients with rtM204 mutation (M:I:V:I/V, no.)	1:14:11:2	1:3:2:1	0:11:8:1
ALT (IU/L), median (range)	86.5 (29–1027)	314.0 (47–760)	78.5 (29–1027)
T. Bil (mg/dL), median (range)	1.1 (0.5–4.5)	1.1 (0.5–1.5)	1.1 (0.5–4.5)
Albumin (g/dL), median (range)	4.1 (2.7–4.8)	4.2 (3.8–4.8)	4.0 (2.7–4.6)
Serum creatinine (mg/dL), median (range)	0.7 (0.4–1.2)	0.7 (0.6–1.2)	0.7 (0.4–1.2)
Prior lamivudine therapy (month), median (range)	28.6 (2–76)	36.5 (2–76)	28.6 (5–65)

HCC, hepatocellular carcinoma; ALT, alanine aminotransferase; T. Bil, total bilirubin. *One patient had genotype A HBV.

Table 2 Virological and biochemical response to lamivudine and adefovir combination therapy during a median of 47 months

	Months of treatment						
Response	0 (n = 28)	6 (n = 28)	12 (n = 27)	24 (n = 25)	36 (n = 22)	48 (n = 13)	60 (n = 7)
HBV DNA < 2.6	0 (0)	11 (39.3)	15 (55.6)	20 (80.0)	19 (86.4)	12 (92.3)	6 (85.7)
HBV DNA 2.6 to <5.0	1 (3.6)	15 (53.6)	11 (40.7)	5 (20.0)	3 (13.6)	1 (7.7)	1 (14.3)
HBV DNA ≥ 5.0	27 (96.4)	2 (7.1)	1 (3.7)	0 (0)	0 (0)	0 (0)	0 (0)
ALT normalization*	NA	16 (57.1)	19 (70.4)	21 (84.0)	18 (81.8)	10 (76.9)	6 (85.7)
HBeAg disappearance†	NA	1/17 (5.9)	4/17 (23.5)	4/16 (25.0)	8/13 (61.5)	7/8 (87.5)	4/5 (80.0)
Virological breakthrough	NA	0 (0)	0 (0)	0 (0)	0 (0)	0 (0)	1 (14.3)

Values are shown as numbers of patients followed by percentages in parentheses. NA, not applicable. *ALT ≤ 35 IU/L. †Values are shown as numbers of patients/total followed by percentages in parentheses.

[5/7 (71%) vs. 5/20 (25%), P = 0.0427]. Although the status of HBeAg at the start of ADV seemed to influence the response, the difference was not significant (Figs 1c,d). Among 17 HBeAg-positive patients, HBeAg disappeared in 6% at 6 months, 24% at 12 months, 25% at 24 months, 62% at 36 months, and 88% at 48 months. There was no patient with hepatitis B surface antigen (HBsAg) loss during follow-up in this study.

Three of 22 patients who were treated for more than 36 months did not achieve virological response. One of them developed virological breakthrough after 54 months of combination therapy. The other patients had 2.8 and 3.5 log copies/mL of serum HBV DNA at 36 months of therapy but did not develop breakthrough. None of the patients experienced biochemical breakthrough. One patient with HCC died of HCC progression at 9 months after ADV. None of the 21 patients without HCC at the start of ADV developed HCC during follow-up.

The renal toxicity with a ≥0.3 mg/dL increase in serum creatinine level was observed in five of the 28 patients. Two of them had a ≥0.5 mg/dL increase: the serum creatinine levels were increased from 0.8 to 1.4 mg/dL after 31 months in a patient, and from 0.9 to 1.7 mg/dL after 34 months in another patient. As their eGFR levels were lowered to 39 and 29 mL/min, the dosage of ADV was reduced to alternate-day administration. After the reduction of ADV, their serum creatinine and eGFR recovered.

Profile of a patient with lamivudine and adefovir dipivoxil resistance

He was a 53-year-old Japanese man with HBeAg-positive liver cirrhosis at the start of 3TC monotherapy in April 2002. The genotype of HBV was found to be genotype C. His clinical course is shown in Fig. 2. He developed breakthrough hepatitis with serum HBV DNA of >7.6 log copies/mL and alanine aminotransferase (ALT) of 236 IU/L in March 2003. ADV was added to the ongoing 3TC therapy in June 2003, and HBV DNA was gradually reduced reaching <2.6 log copies/mL 3 years later. However, virological

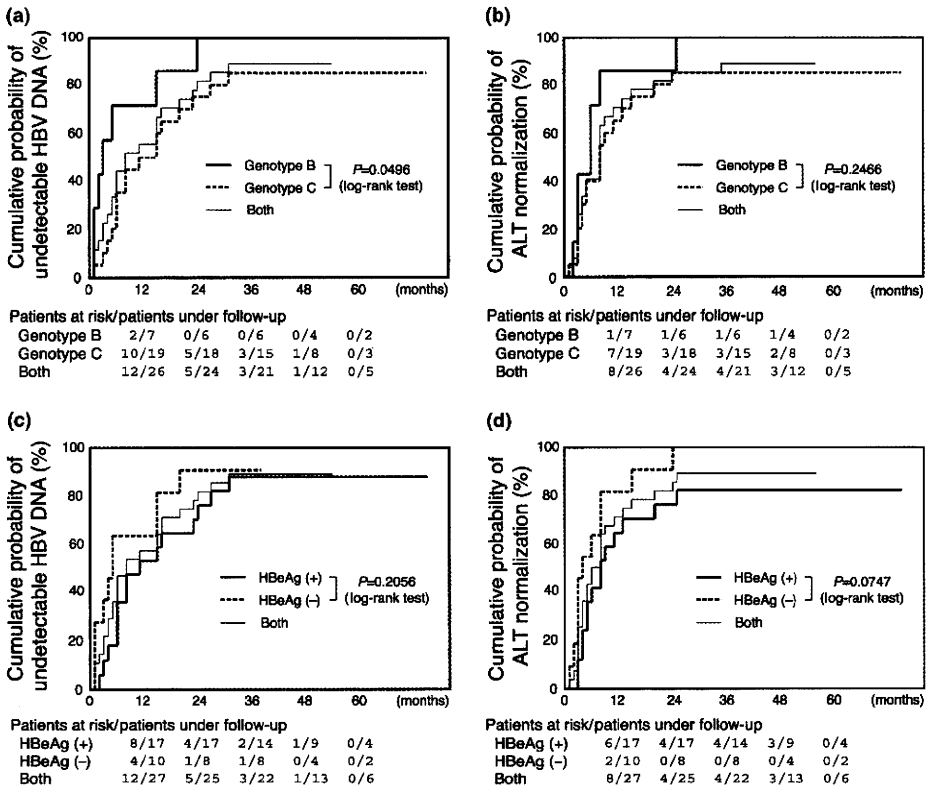

Fig. 1 Cumulative probability of virological or biochemical response during lamivudine (3TC) and adefovir dipivoxil (ADV) combination therapy. (a) Cumulative probability of undetectable HBV DNA (<2.6 log copies/mL) in patients with genotype B and those with genotype C. (b) Cumulative probability of ALT normalization (≤35 IU/L) in patients with genotype B and those with genotype C. (c) Cumulative probability of undetectable HBV DNA in HBeAg-positive patients and HBeAg-negative patients. (d) Cumulative probability of ALT normalization in HBeAg-positive patients and HBeAg-negative patients.

breakthrough was observed at 4 years after starting ADV, and his HBV DNA reached 4.3 log copies/mL in December 2007. Because his liver was cirrhotic and the hepatic functional reserve was impaired, combination therapy of tenofovir disoproxil fumarate (TDF) and 3TC was started before ALT flair. Two months later, his HBV DNA was suppressed to <2.6 log copies/mL, and viral breakthrough has not been observed to date (20 months later).

Mutations found in the HBV reverse transcriptase region of the lamivudine and adefovir dipivoxil-resistant patient

To investigate the mutations responsible for the viral breakthrough during the 3TC and ADV combination therapy, nucleotide sequences of the HBV RT region of the patient were compared between 3 time points: at the beginning of ADV treatment, at 30 months after ADV therapy, and at the time of viral breakthrough (54 months after ADV therapy). Direct sequencing analysis showed 10 amino acid changes during the clinical course (Fig. 2). The 3TC-resistant mutation of rtM204I changed to rtM204V after ADV treatment. Along with the change, the mixed mutation of rtL180L/M changed to rtL180M, which was reported to emerge with rtM204V during 3TC therapy [9]. The rtN236T mutation, which is a known ADV-resistance mutation [11], emerged as a mixed mutation with wild type (rtN236N/T) after viral breakthrough. Notably, rtA200V, which has never been reported as an ADV-resistant mutation, emerged also after viral breakthrough as a mixed mutation (rtA200V/A). Meanwhile, no specific mutation was found in the 2 patients without virological breakthrough who did not achieve virological response after 3 years of the combination therapy.

Clonal analysis was performed to examine the significance of these mutations of the RT region (Table S1). Several minor mutations were found during the 3TC and ADV therapy. After viral breakthrough, rtA200V was found in 63% of the clones, while rtN236T was found in only 25% of the clones. Therefore, rtA200V seemed to be responsible for the treatment failure of ADV. Moreover, rtT184S and S202C, which were reported as ETV resistance–associated mutations [29], were found as a minor population.

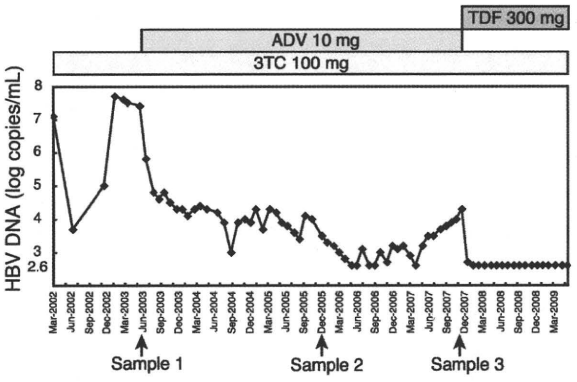

RT mutation	L80	P109	D134	R153	L180	A200	M204	V214	L229	N236
Sample 1	I/L	P/Q	G/D	R/Q	L/M	–	I	–	L/W	–
Sample 2	–	–	–	–	M	–	V	A	–	–
Sample 3	–	–	G/D	–	M	V/A	V	–	–	N/T

Fig. 2 Clinical course of a lamivudine (3TC)-resistant patient who developed virological breakthrough during 3TC and adefovir dipivoxil (ADV) combination therapy, and changes of amino acids in the reverse transcriptase (RT) region detected by direct sequencing analysis. After breakthrough, therapy was switched to 3TC plus tenofovir disoproxil fumarate (TDF) combination. The arrows indicate the time point when serum samples were obtained for sequencing analysis. Sample 1, 2, and 3 were obtained at the start of ADV, 30 months after ADV, and 54 months after ADV, respectively.

To investigate further the mutant populations, the combinations of these mutations and 3TC-resistant mutations were analysed (Fig. 3). At 30 months after ADV therapy, 100% of clones had mutations rtL180M+M204V. Subsequently, the mutations of rtT184S, A200V, S202C, and N236T emerged in the rtL180M+M204V clones after viral breakthrough. Of note, rtN236T was not found in clones without rtA200V.

Replication capacity and drug susceptibility of HBV mutants

We analysed the replication capacity of HBV clones with combined mutations as shown in Fig. 3. A clone with rtL180M+M204V+N236T mutations, which was not found in the patient, was also included for comparison. Consistent with a previous report [30], 3TC-resistant mutations of rtM204I or rtL180M+M204V lowered the replication capacity significantly in comparison with the wild-type clone (Table 3). From additional mutations to rtL180M+M204V found in the patient, only rtA200V restored the impaired replication capacity significantly. The ETV-resistant mutation of rtT184S and rtS202C did not seem to have such an effect. The ADV-resistant mutation, rtN236T, lowered the replication capacity further, and rtA200V did not restore the lowered capacity caused by rtN236T.

The 7 HBV clones with mutations in the RT region were analysed for their susceptibility to ADV. The IC_{50} of each clone is shown in Table 3. The clones with the 3TC-resistant mutations of rtM204I or rtL180M+M204V showed moderate resistance to ADV. In comparison with the clone with rtL180M+M204V, clones with additional mutations of rtT184S, A200V, or S202C showed significantly higher resistance to ADV. An additional mutation of rtN236T led to much greater resistance to ADV. Taking into account the results from the clonal analysis of serum samples and the replication capacity of each clone, rtA200V may be responsible for the treatment failure of 3TC+ADV therapy when it presents with 3TC-resistant mutations such as rtL180M+M204V. The mutations of rtT184S or S202C with rtL180M+M204V also confer ADV resistance, but the clones

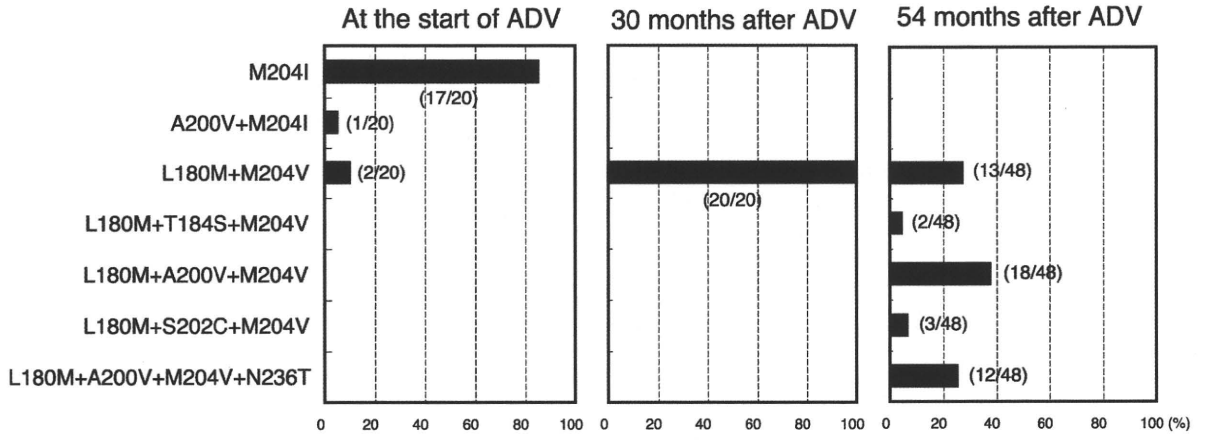

Fig. 3 Clonal analysis of HBV obtained from the patient with 3TC and ADV resistance. The serum samples were collected at the time points indicated in Fig. 2. The percentages (no. of clones/total in parentheses) of the clones with the combined mutations in the RT region are shown.

Table 3 Replication capacity and susceptibility to adefovir of the HBV mutants

HBV mutants	HBV DNA ($\times 10^7$ log copies/mL)*	Fold replication†	IC_{50} (μM)*	Fold resistance†
Wild type	13.60 ± 3.50	1	0.42 ± 0.06	1
M204I	2.17 ± 0.38	0.16	0.87 ± 0.2	2.07
L180M+M204V	4.38 ± 0.77	0.32	0.73 ± 0.06	1.74
L180M+T184S+M204V	5.98 ± 0.80	0.44	0.91 ± 0.04	2.17‡
L180M+A200V+M204V	8.90 ± 0.56	0.65‡	1.09 ± 0.12	2.60‡
L180M+S202C+M204V	4.86 ± 0.19	0.36	2.19 ± 0.63	5.21‡
L180M+M204V+N236T	0.88 ± 0.68	0.07‡	>10	>25
L180M+A200V+M204V+N236T	0.54 ± 0.38	0.04‡	>10	>25

*Values are expressed as means ± SD of experiments performed in triplicate. †(Mean value of the mutant)/(mean value of the wild type). ‡$P < 0.05$ in comparison with the clone with rtL180M+M204V.

with these mutations were not major, because they had no effect in enhancing the replication capacity of HBV.

DISCUSSION

As clinical and histological improvement accompanies reductions in HBV replication, therapies that reduce HBV replication are expected to limit the progression of liver disease and improve the natural history of chronic HBV infection [10]. Currently, the management of hepatitis B patients with drug resistance is one of the major problems in clinical practice for hepatitis B. A substantial part of 3TC-treated patients has mutant HBV with the YMDD mutation, and several clinical trials to treat 3TC-resistant hepatitis B have been performed. It has been reported first that with ADV alone and in combination with 3TC, the viral and biochemical responses were the same for 3TC-resistant patients in a 1 year study [31]. However, several studies of longer term treatment have shown that adding ADV was superior to switching to ADV monotherapy for patients with 3TC resistance [32–34]. In this study, we demonstrated that the add-on ADV therapy for 3TC-resistant hepatitis B patients effectively suppressed serum HBV DNA for a median of 47 months. Moreover, the biochemical response of ALT normalization was achieved in 77% patients and HBeAg loss in 88% of the HBeAg-positive patients at 48 months. The undetectability of HBV DNA was assessed by the Amplicor HBV monitor test, but recently, this can be assessed by a more sensitive real-time assay such as the Cobas TaqMan HBV test (Roche Diagnostics). The treatment duration to achieve HBV DNA undetectability might be longer if a more sensitive assay was used.

The influence of HBV genotype on the response or resistance to ADV has not been clarified, whereas the efficacy to 3TC was reported to be different between HBV genotypes [24,25]. This study showed that the virological response to 3TC+ADV was significantly earlier in genotype B than in C. However, there were several limitations of the results: the patients with genotype B were fewer, and no multivariate analysis was performed. In addition, all patients with HCC were genotype C, and ALT levels of genotype B tended to be higher, although there were no significant differences. The effect of genotype on the response to 3TC±ADV should be confirmed in larger studies. The baseline HBeAg status in 3TC+ADV combination therapy in 3TC-resistant patients was reported to influence the viral response: HBeAg-negative patients showed better virological and biological response [35]. In this study, the same tendency was observed, but the difference was not significant.

Initial virological suppression by ADV monotherapy was reported to be a good prognostic factor for the treatment of both naïve patients [36] and 3TC-resistant patients [37]. Taking into account the results of this study and previous reports, it is suggested that patients with genotype B HBV might develop resistance to 3TC+ADV less frequently than those with genotype C. In fact, the 3TC+ADV-resistant patient in this study was infected with genotype C HBV. Because the development of resistance to 3TC+ADV combination therapy is rare [22,35], it is difficult to evaluate whether the early virological response or genotype B is associated with the lower frequency of resistance to 3TC+ADV combination therapy. Further long-term study is needed to clarify this issue.

Although the emergence of resistance in this study was rare during the combination therapy as previously reported [22,35], one patient developed virological breakthrough after 4.5 years. We identified a characteristic mutation pattern of HBV in this patient. The mutation of rtA200V rescued the *in vitro* replication capacity that was impaired by rtL180M+M204V and reduced the susceptibility to ADV. In previous reports, rtA200V emerged as an additional mutation with the 3TC-resistant mutation in patients under 3TC monotherapy [38,39]. The effect of this mutation is not as strong as the effect of rtM204I/V±L180M on 3TC susceptibility *in vitro*, which showed >1000-fold resistance [40]. However, the clinical dose of ADV is comparatively low

because of renal toxicity [41], and the weakly resistant profile *in vitro* can explain the great clinical impact. Villet *et al.* reported that rtA200V was observed in a patient with 3TC monotherapy, and it was no longer detected after the combination therapy with ADV and 3TC [39]. The difference of results between the previous study and our study may be because of the emergence of mutations with a potent effect on ADV resistance, such as rtV173L and rtA181V, in the previous study. Because these mutations may have a greater effect on ADV resistance than rtA200V, the HBV clones with rtA200V seemed to disappear in the previous study case.

The known ADV-resistant mutation of rtN236T was found in only 25% clones, exclusively with rtA200V. This may indicate that rtN236T appeared after the emergence of rtA200V. In the active replication of the clones with rtA200V, which restored the replication capacity and enhanced ADV resistance, other mutations including rtN236T might occur more readily.

The rtA200V mutation is the result of nucleotide substitution C728T. This change in the overlapping S region results in an amino acid substitution affecting HBsAg: Leu to Phe at aa192 (sL192F). There is a possibility that sL192F may affect the replication capacity of HBV, but the actual mechanism is unknown.

Interestingly, the ETV-resistant mutations of rtT184S and rtS202C were also detected during 3TC+ADV combination therapy by clonal analysis. These mutations confer ETV resistance in the presence of the 3TC-resistant mutations of rtM204I/V±L180M [21]. This study showed that these mutations also have an ADV-resistance profile. These mutations may not cause viral breakthrough, because the population of these mutants in the patient was minor (4% and 6%, respectively), and their replication capacity was lower than that with rtA200V *in vitro*. The emergence of these mutations suggested that long-term 3TC+ADV therapy has the possibility of leading to multiple drug resistance including ETV resistance.

The combination therapy of 3TC and ADV is very effective with little frequency of viral breakthrough for 3TC-refractory patients. However, some patients do not achieve complete viral suppression of serum HBV DNA to under 2.6 log copies/mL. It was considered that the incomplete suppression of viral replication might favour further selection of drug-resistant mutants [42]. Although there have been a few reports of cases that showed resistance to 3TC+ADV therapy to date, the number of resistant cases will increase along with the increase in cases with long-term therapy. The 3TC- and ADV-resistant patient in this study was treated with 3TC and TDF after the virological breakthrough, and HBV DNA was promptly suppressed. Although TDF was reported to show cross-resistance with ADV *in vitro* [16,40,43], there are several reports that showed the effectiveness of TDF for ADV-refractory patients [44–46]. It is thought that the potency of TDF might result from its higher clinical dose compared to that of ADV [47].

In conclusion, this study showed that the combination therapy of 3TC and ADV effectively suppressed HBV replication in 3TC-resistant patients with chronic HBV infection for 4 years. Especially, patients with genotype B achieved earlier virological response than those with genotype C. However, one of the 28 patients developed virological breakthrough during the combination therapy over 4 years, and the HBV mutation of rtA200V, in addition to 3TC-resistant mutations, was demonstrated to contribute to the ADV resistance. Moreover, ETV-resistant mutations emerged coincidentally in minor HBV clones. The risk of emergence of multiple drug-resistant mutant should be considered in cases with long-term therapy with nucleos(t)ide analogues, especially when serum HBV DNA cannot be suppressed completely. Potent antiviral agents should be administered in such cases to prevent the emergence of multiple drug-resistant HBV mutants that are difficult to treat.

ACKNOWLEDGEMENTS

This study was supported in part by Grant-in-Aid for Young Scientists (B) (assignment no. 20790483) from Ministry of Education, Culture, Sports, Science, and Technology of Japan, and by grants from Ministry of Health, Labor, and Welfare of Japan.

REFERENCES

1 Ganem D, Prince AM. Hepatitis B virus infection – natural history and clinical consequences. *N Engl J Med* 2004; 350: 1118–1129.
2 Doong SL, Tsai CH, Schinazi RF, Liotta DC, Cheng YC. Inhibition of the replication of hepatitis B virus in vitro by 2′,3′-dideoxy-3′-thiacytidine and related analogues. *Proc Natl Acad Sci U S A* 1991; 88: 8495–8499.
3 Lai CL, Chien RN, Leung NW *et al.* A one-year trial of lamivudine for chronic hepatitis B. Asia Hepatitis Lamivudine Study Group. *N Engl J Med* 1998; 339: 61–68.
4 Ling R, Mutimer D, Ahmed M *et al.* Selection of mutations in the hepatitis B virus polymerase during therapy of transplant recipients with lamivudine. *Hepatology* 1996; 24: 711–713.
5 Lai CL, Dienstag J, Schiff E *et al.* Prevalence and clinical correlates of YMDD variants during lamivudine therapy for patients with chronic hepatitis B. *Clin Infect Dis* 2003; 36: 687–696.
6 Zoulim F. Hepatitis B virus resistance to antivirals: clinical implications and management. *J Hepatol* 2003; 39(Suppl. 1): S133–S138.
7 Tipples GA, Ma MM, Fischer KP, Bain VG, Kneteman NM, Tyrrell DL. Mutation in HBV RNA-dependent DNA polymerase confers resistance to lamivudine *in vivo*. *Hepatology* 1996; 24: 714–717.
8 Delaney IV WE, Yang H, Westland CE *et al.* The hepatitis B virus polymerase mutation rtV173L is selected during lamivudine therapy and enhances viral replication in vitro. *J Virol* 2003; 77: 11833–11841.

9 Ono SK, Kato N, Shiratori Y *et al.* The polymerase L528M mutation cooperates with nucleotide binding-site mutations, increasing hepatitis B virus replication and drug resistance. *J Clin Invest* 2001; 107: 449–455.

10 Dienstag JL. Hepatitis B virus infection. *N Engl J Med* 2008; 359: 1486–1500.

11 Angus P, Vaughan R, Xiong S *et al.* Resistance to adefovir dipivoxil therapy associated with the selection of a novel mutation in the HBV polymerase. *Gastroenterology* 2003; 125: 292–297.

12 Villeneuve JP, Durantel D, Durantel S *et al.* Selection of a hepatitis B virus strain resistant to adefovir in a liver transplantation patient. *J Hepatol* 2003; 39: 1085–1089.

13 Fung SK, Andreone P, Han SH *et al.* Adefovir-resistant hepatitis B can be associated with viral rebound and hepatic decompensation. *J Hepatol* 2005; 43: 937–943.

14 Hadziyannis SJ, Tassopoulos NC, Heathcote EJ *et al.* Long-term therapy with adefovir dipivoxil for HBeAg-negative chronic hepatitis B. *N Engl J Med* 2005; 352: 2673–2681.

15 Hadziyannis SJ, Tassopoulos NC, Heathcote EJ *et al.* Long-term therapy with adefovir dipivoxil for HBeAg-negative chronic hepatitis B for up to 5 years. *Gastroenterology* 2006; 131: 1743–1751.

16 Brunelle MN, Jacquard AC, Pichoud C *et al.* Susceptibility to antivirals of a human HBV strain with mutations conferring resistance to both lamivudine and adefovir. *Hepatology* 2005; 41: 1391–1398.

17 Papatheodoridis GV, Manolakopoulos S, Dusheiko G, Archimandritis AJ. Therapeutic strategies in the management of patients with chronic hepatitis B virus infection. *Lancet Infect Dis* 2008; 8: 167–178.

18 Lau DT, Khokhar MF, Doo E *et al.* Long-term therapy of chronic hepatitis B with lamivudine. *Hepatology* 2000; 32: 828–834.

19 Westland CE, Yang H, Delaney IV WE *et al.* Activity of adefovir dipivoxil against all patterns of lamivudine-resistant hepatitis B viruses in patients. *J Viral Hepat* 2005; 12: 67–73.

20 Chang TT, Gish RG, Hadziyannis SJ *et al.* A dose-ranging study of the efficacy and tolerability of entecavir in Lamivudine-refractory chronic hepatitis B patients. *Gastroenterology* 2005; 129: 1198–1209.

21 Tenney DJ, Levine SM, Rose RE *et al.* Clinical emergence of entecavir-resistant hepatitis B virus requires additional substitutions in virus already resistant to Lamivudine. *Antimicrob Agents Chemother* 2004; 48: 3498–3507.

22 Lampertico P, Vigano M, Manenti E, Iavarone M, Sablon E, Colombo M. Low resistance to adefovir combined with lamivudine: a 3-year study of 145 lamivudine-resistant hepatitis B patients. *Gastroenterology* 2007; 133: 1445–1451.

23 Tenney DJ, Rose RE, Baldick CJ *et al.* Long-term monitoring shows hepatitis B virus resistance to entecavir in nucleoside-naive patients is rare through 5 years of therapy. *Hepatology* 2009; 49: 1503–1514.

24 Orito E, Fujiwara K, Tanaka Y *et al.* A case-control study of response to lamivudine therapy for 2 years in Japanese and Chinese patients chronically infected with hepatitis B virus of genotypes Bj, Ba and C. *Hepatol Res* 2006; 35: 127–134.

25 Kobayashi M, Suzuki F, Akuta N *et al.* Response to long-term lamivudine treatment in patients infected with hepatitis B virus genotypes A, B, and C. *J Med Virol* 2006; 78: 1276–1283.

26 Levey AS, Bosch JP, Lewis JB, Greene T, Rogers N, Roth D. A more accurate method to estimate glomerular filtration rate from serum creatinine: a new prediction equation. Modification of Diet in Renal Disease Study Group. *Ann Intern Med* 1999; 130: 461–470.

27 Takahashi M, Nishizawa T, Gotanda Y *et al.* High prevalence of antibodies to hepatitis A and E viruses and viremia of hepatitis B, C, and D viruses among apparently healthy populations in Mongolia. *Clin Diagn Lab Immunol* 2004; 11: 392–398.

28 Inoue J, Ueno Y, Nagasaki F *et al.* Enhanced intracellular retention of a hepatitis B virus strain associated with fulminant hepatitis. *Virology* 2009; 395: 202–209.

29 Tenney DJ, Rose RE, Baldick CJ *et al.* Two-year assessment of entecavir resistance in Lamivudine-refractory hepatitis B virus patients reveals different clinical outcomes depending on the resistance substitutions present. *Antimicrob Agents Chemother* 2007; 51: 902–911.

30 Melegari M, Scaglioni PP, Wands JR. Hepatitis B virus mutants associated with 3TC and famciclovir administration are replication defective. *Hepatology* 1998; 27: 628–633.

31 Peters MG, Hann HW, Martin P *et al.* Adefovir dipivoxil alone or in combination with lamivudine in patients with lamivudine-resistant chronic hepatitis B. *Gastroenterology* 2004; 126: 91–101.

32 Gaia S, Barbon V, Smedile A *et al.* Lamivudine-resistant chronic hepatitis B: an observational study on adefovir in monotherapy or in combination with lamivudine. *J Hepatol* 2008; 48: 540–547.

33 Fung SK, Chae HB, Fontana RJ *et al.* Virologic response and resistance to adefovir in patients with chronic hepatitis B. *J Hepatol* 2006; 44: 283–290.

34 Rapti I, Dimou E, Mitsoula P, Hadziyannis SJ. Adding-on versus switching-to adefovir therapy in lamivudine-resistant HBeAg-negative chronic hepatitis B. *Hepatology* 2007; 45: 307–313.

35 Yatsuji H, Suzuki F, Sezaki H *et al.* Low risk of adefovir resistance in lamivudine-resistant chronic hepatitis B patients treated with adefovir plus lamivudine combination therapy: two-year follow-up. *J Hepatol* 2008; 48: 923–931.

36 Gallego A, Sheldon J, Garcia-Samaniego J *et al.* Evaluation of initial virological response to adefovir and development of adefovir-resistant mutations in patients with chronic hepatitis B. *J Viral Hepat* 2008; 15: 392–398.

37 Chan HL, Wong VW, Tse CH *et al.* Early virological suppression is associated with good maintained response to adefovir dipivoxil in lamivudine resistant chronic hepatitis B. *Aliment Pharmacol Ther* 2007; 25: 891–898.

38 Zollner B, Petersen J, Puchhammer-Stockl E *et al.* Viral features of lamivudine resistant hepatitis B genotypes A and D. *Hepatology* 2004; 39: 42–50.

39 Villet S, Pichoud C, Villeneuve JP, Trepo C, Zoulim F. Selection of a multiple drug-resistant hepatitis B virus strain in a liver-transplanted patient. *Gastroenterology* 2006; 131: 1253–1261.

40 Shaw T, Bartholomeusz A, Locarnini S. HBV drug resistance: mechanisms, detection and interpretation. *J Hepatol* 2006; 44: 593–606.
41 Marcellin P, Chang TT, Lim SG *et al.* Adefovir dipivoxil for the treatment of hepatitis B e antigen-positive chronic hepatitis B. *N Engl J Med* 2003; 348: 808–816.
42 Santantonio T, Fasano M, Durantel S *et al.* Adefovir dipivoxil resistance patterns in patients with lamivudine-resistant chronic hepatitis B. *Antivir Ther* 2009; 14: 557–565.
43 Qi X, Xiong S, Yang H, Miller M, Delaney WE. In vitro susceptibility of adefovir-associated hepatitis B virus polymerase mutations to other antiviral agents. *Antivir Ther* 2007; 12: 355–362.
44 Tan J, Degertekin B, Wong SN, Husain M, Oberhelman K, Lok AS. Tenofovir monotherapy is effective in hepatitis B patients with antiviral treatment failure to adefovir in the absence of adefovir-resistant mutations. *J Hepatol* 2008; 48: 391–398.
45 van Bommel F, Zollner B, Sarrazin C *et al.* Tenofovir for patients with lamivudine-resistant hepatitis B virus (HBV) infection and high HBV DNA level during adefovir therapy. *Hepatology* 2006; 44: 318–325.
46 Choe WH, Kwon SY, Kim BK *et al.* Tenofovir plus lamivudine as rescue therapy for adefovir-resistant chronic hepatitis B in hepatitis B e antigen-positive patients with liver cirrhosis. *Liver Int* 2008; 28: 814–820.
47 Lok AS, McMahon BJ. Chronic hepatitis B. *Hepatology* 2007; 45: 507–539.

SUPPORTING INFORMATION

Additional Supporting Information may be found in the online version of this article:

Table S1 Clonal analysis of HBV RT region of samples from the patient with lamivudine and adefovir resistance.

Please note: Wiley-Blackwell are not responsible for the content or functionality of any supporting materials supplied by the authors. Any queries (other than missing material) should be directed to the corresponding author for the article.

Biochemical and Biophysical Research Communications 399 (2010) 384–390

Contents lists available at ScienceDirect

Biochemical and Biophysical Research Communications

journal homepage: www.elsevier.com/locate/ybbrc

Exosome secretion of dendritic cells is regulated by Hrs, an ESCRT-0 protein

Keiichi Tamai [a,b,d], Nobuyuki Tanaka [c,d,*], Takashi Nakano [e], Eiji Kakazu [b], Yasuteru Kondo [b], Jun Inoue [b], Masaaki Shiina [b], Koji Fukushima [b], Tomoaki Hoshino [f], Kouichi Sano [e], Yoshiyuki Ueno [b], Tooru Shimosegawa [b], Kazuo Sugamura [a,d]

[a] Department of Microbiology and Immunology, Tohoku University Graduate School of Medicine, Sendai 980-8575, Japan
[b] Department of Gastroenterology, Tohoku University Graduate School of Medicine, Sendai 980-8575, Japan
[c] Department of Cancer Science, Tohoku University Graduate School of Medicine, Sendai 980-8575, Japan
[d] Division of Immunology, Miyagi Cancer Center Research Institute, Natori, Miyagi 981-1293, Japan
[e] Department of Preventive and Social Medicine, Osaka Medical College, Takatsuki, Osaka 569-8686, Japan
[f] Division of Respirology, Neurology, and Rheumatology, Department of Medicine, Kurume University School of Medicine, 67 Asahi-machi, Kurume 830-0011, Japan

ARTICLE INFO

Article history:
Received 16 July 2010
Available online 29 July 2010

Keywords:
Dendritic cells
ESCRT
Exosomes
Hrs

ABSTRACT

Exosomes are nanovesicles derived from multivesicular bodies (MVBs) in antigen-presenting cells. The components of the ESCRT (endosomal sorting complex required for transport) pathway are critical for the formation of MVBs, however the relationship between the ESCRT pathway and the secretion of exosomes remains unclear. We here demonstrate that Hrs, an ESCRT-0 protein, is required for fascilitating the secretion of exosomes in dendritic cells (DCs). Ultrastructural analyses showed typical saucer-shaped exosomes in the culture supernatant from both the control and Hrs-depleted DCs. However, the amount of exosome secretion was significantly decreased in Hrs-depleted DCs following stimulations with ovalbumin (OVA) as well as calcium ionophore. Antigen-presentation activity was also suppressed in exsosomes purified from Hrs-depleted DCs, while no alteration in OVA degradation was seen in Hrs-depleted DCs. These data indicated that Hrs is involved in the regulation of antigen presentation activity through the exosome secretion.

1. Introduction

Exosomes are nanovesicles (60–90 nm in diameter) surrounded by a lipid bilayer. Exosomes are secreted from a variety of cells, including antigen-presenting cells (APCs), B cells, monocytes, and dendritic cells (DCs) [1], in physiological situations. They are generated as the intraluminal vesicles (ILVs) of a sorting endosome called a multivesicular body (MVB), by the inward budding of the MVB's limiting membrane. The release of exosomes into the extracellular milieu is achieved by the direct fusion of the MVB with the plasma membrane. Exosomes possess selected cargo proteins originating from the MVB membrane, including the major histocompatibility complex (MHC), costimulatory molecules, tetraspanins, adhesion molecules, and cytosolic proteins, and the biological functions of exosomes depend mainly on the types of cargo proteins they contain. For instance, APC-derived exosomes are capable of directly sensitizing naïve T cells via the MHC/peptide complex and the costimulatory molecules on their surface [2]. On the other hand, exosome like vesicles secreted from intestinal epithelial cells can induce tolerance in an antigen peptide-specific manner [3,4]. These findings suggest that exosomes carrying MHC proteins can regulate immune responses positively or negatively in vivo.

Exosomes also contain ubiquitinated proteins, suggesting that a subset of ubiquitinated cytoplasmic proteins is actively incorporated into the MVB pathway [5]. The sorting of ubiquitinated proteins on MVBs is mediated by a series of proteins involved in vacuolar protein sorting (VPS), called endosomal sorting complex required for transport (ESCRT). The first complex that binds the cargo on endosomes is ESCRT-0 (it includes Hrs [6,7] and STAM), and with the help of the ESCRTs-I, -II, and –III, the cargo accumulates on the endosomal membrane. At the end of the sorting, an AAA-type ATPase, VPS4, disrupts the ESCRT complexes, and the membrane with its accumulated cargo is invaginated into the maturing endosome to produce an intraluminal vesicle, called an MVB. Most of the ubiquitinated cargo, which includes epithelial growth factor (EGF) receptors, c-Met, and gp130, is degraded by lysosomal proteases. A deficiency of Hrs results in abnormally enlarged endosomes

Abbreviations: APC, antigen-presenting; ESCRT, endosomal sorting complex required for transport; ILV, intraluminal vesicle; MVB, multivesicular body; MHC, major histocompatibility complex; N-Rh-PE, N-(lissamine rhodamine B sulfonyl) phosphatidyl ethanolamine; OVA, ovalbumin; TEM, transmission electron microscopy; VPS, vacuolar protein sorting.

* Corresponding author at: Division of Immunology, Miyagi Cancer Center Research Institute, 47-1 Nodayama, Medeshima-Shiode, Natori, Miyagi 981-1293, Japan. Fax: +81 22 381 1168.
E-mail address: tanaka@med.tohoku.ac.jp (N. Tanaka).

0006-291X/$ - see front matter © 2010 Elsevier Inc. All rights reserved.
doi:10.1016/j.bbrc.2010.07.083

and a marked reduction in cargo sorting to the MVBs, which accumulate ligand-activated membrane-bound growth factor receptors [8]. While most of the cargo is destined for degradation, some MVBs direct their ILVs to be secreted as exosomes by direct fusion with the plasma membrane [9]. In this context, the intracellular membrane traffic system seems to play key role in the formation and release of exosomes. Previous studies suggested that at least four Rab GTPase members, Rab5, Rab11, Rab27a and Rab27b are involved in the secretion of exosomes [10–12]. Nevertheless, the precise mechanisms of the exosome pathway are still unclear.

Considering that the importance of MVB formation in exosomal pathway, as well as the presence of ubiquitinated proteins in exosomes, we suspected that Hrs might be involved in exosomal pathway. We report here that Hrs is required for secretion of exosomes in DCs.

2. Materials and Methods

2.1. Ethics Statements

This study was conducted according to the principles expressed in the Declaration of Helsinki and Fundamental Guidelines for Animal Experiments and Related Activities. The study was approved by the research committees of the Miyagi Cancer Center and Tohoku University. All the animal experiments were conducted under the approval of the Institutional Animal Care and Use Committees of Miyagi Cancer Center and Tohoku University.

2.2. Cells

DC2.4 cells (murine DC line) were maintained in RPMI medium containing 10% fetal calf serum, 2 mM L-glutamine, 1 mM sodium pyruvate, 0.1 mM non-essential amino acids, 10 mM hepes buffer, and antibiotics. We also generated primary DCs from mouse bone marrow using a standard method, as previously described [13]. To express Hrs-specific short hairpin RNA (shRNA), a retroviral vector (pSIREN-RetroQ, BD Biosciences) was generated as described previously [14]. The target sequence consisted of nucleotide residues 302–320 (5′-AGG TAA ACG TCC GTA ACA A-3′) in the human hrs cDNA. A control plasmid, pSIREN-RetroQ-Luc, targeted bp 413–434 of firefly luciferase (5′-GCA ATA GTT CAC GCT GAA AAG-3′). The retrovirus was prepared as previously described [14].

2.3. Mice

We generated a conditional knock-out of Hrs as described previously (Acc. No. CDB0476 K, Center for Developmental Biology, Kobe, Japan) [15]. To generate a dendritic-cell-specific conditional knockout of Hrs, We crossed this mouse with a LysM-cre transgenic mouse (a gift from Dr. I. Foerster) [16]. The OT-I TCR-transgenic mice were a gift from Dr. W. Heath (Walter and Eliza Hall Institute, Melbourne, Australia) and were used as the source of $CD8^+$ T cells that were specifically responsive to the OVA257–264 peptide [17].

2.4. Genotype analysis

The *hrs flox* allele was genotyped as described previously [15]. Genotyping for the presence of the LysM-Cre allele was performed using the following primer pair: forward (5′-TTA CCG GTC GAT GCA ACG AGT GAT G) and reverse (5′-TTC CAT GAG TGA ACG AAC CTG GTC G).

2.5. Isolation and purification of exosomes

Exosomes were purified as previously described [2,18]. In brief, the cell culture medium was centrifuged for 10 min at 300 g, 10 min at 1200 g, and 30 min at 10,000 g to remove the cells and debris. The supernatant obtained from the last spin was then centrifuged for 60 min at 100,000 g, and the pellet was solubilized in SDS sample buffer for analyses by Western blotting.

2.6. Fluorescent N-Rh-PE measurement

To measure exosome secretion, the fluorescent phospholipid analog N-(lissamine rhodamine B sulfonyl) phosphatidyl ethanolamine (N-Rh-PE) was inserted into the plasma membrane as described previously [19], and eventually secreted into the extracellular medium [10]. Briefly, the lipid was solubilized in absolute ethanol and injected into serum-free RPMI (<1% v/v) during vigorous vortexing. The mixture was then added to the cells, which were incubated for 60 min at 4 °C. After this incubation, the medium was removed, and the cells were extensively washed with cold PBS. The labeled cells were cultured in complete RPMI medium to collect the exosomes. To measure the exosome secretion, 50 μl of the exosomal fraction was solubilized in 1.5 ml PBS containing 0.1% Triton X-100, and the N-Rh-PE was measured at 560 nm and 590 nm excitation and emission wavelengths, respectively.

2.7. OVA protein degradation

Control and Hrs-depleted dendritic cell lines were treated with a lysosomal inhibitor (50 mM NH_4Cl) and/or proteasomal inhibitor (10 μM epoxomicin) for up to 2 h. The cells were pulsed with 300 μg/ml ovalbumin (OVA) protein for 1 h, and incubated with fresh medium for the indicated times. For western blot analysis, an anti-OVA antibody (rabbit polyclonal antibody, Abnova, Taiwan) was used for the first antibody.

2.8. Western blotting

Immunoblotting was carried out as described previously [20]. For dot-blot analysis, each cell lysate was spotted onto PVDF membranes.

2.9. Phenotypic analysis of cells by flow cytometry

Cells were assessed for surface marker expression by fluorescent multicolor flow cytometry (FACSCalibur, Becton Dickinson, San Jose, CA). The immunophenotypic profile of DCs was evaluated by staining with anti-CD40, anti-CD80, anti-I-$A^β$, and anti-H-2 $K^β$ antibodies (Pharmingen).

2.10. Antigen presentation assays

To assess the function of DC-derived exosomes, we performed an in vitro $CD8^+$ T-cell proliferation assay as described previously [21]. The spleen was harvested from OT-I mice, and the $CD8^+$ T cells were positively selected using MACS magnetic beads (Miltenyi Biotec). Next, 4×10^6 BMDCs from $Hrs^{+/+}$; LysM-Cre and $Hrs^{flox/flox}$; LysM-Cre mice were incubated with 300 mg/ml OVA for 24 h. Exosomes in 10 ml of supernatant were purified as described above. The purified OT-I $CD8^+$ T cells were cocultured with the purified exosomes in 96-well plates for 5 days. The exosome induced proliferation of the OT-I T cells was measured after 5 days by adding [^{3}H]thymidine (1 μCi/well; ICN Pharmaceuticals) during the last 8 h of each culture.

2.11. Negative staining in electron microscopy

Samples of exosomes pelletted by ultracentrifugation as described above were resuspended in 0.1% glutaraldehyde, and a

drop of each resuspension was mounted on an ion-coated copper grid supported by a carbon-coated collodion film. The grid was stained with 1% uranyl acetate for 1 min and observed under an electron microscope (H-7650, Hitachi, Tokyo, Japan).

3. Results

3.1. Establishment of Hrs-depleted DCs and purification of exosomes

To examine the role of Hrs in exosome secretion, we established an Hrs-depleted dendritic cell (DC) line through retrovirus-mediated shRNA expression (Fig. 1A). The exosome-containing fractions were purified from the DCs by sucrose gradient centrifugation, using an anti-MHC-class II (I-A^{β}) antibody to detect the exosomes. The fraction containing the peak I-A^{β}-binding activity occurred at 1.15 g/ml sucrose in the sample from control DCs, and 1.14 g/ml from the Hrs-depleted DCs, indicating a similar distribution irrespective of the Hrs expression (Fig. 1B). Although these values were slightly different, they were both within the normal density profile for DC-derived exosomes in sucrose gradients [22]. Ultrastructural analysis of the ultracentrifuged exosome pellets by negative stain method of transmission electron microscopy (TEM) showed them to be markedly enriched in typical saucer-shaped exosomes, 40–100 nm in diameter, from both the control and knock-out DCs (Fig. 1C).

We further examined the exosome-containing fractions by Western blot analysis. Exosomes from the Hrs-depleted DCs under steady-state conditions contained less ubiquitinated protein than exosomes from control DCs, although the total ubiquitinated protein in the whole-cell lysates of both types of DCs was the same (Fig. 1D). MHC-I and -II, two marker proteins for DC-derived exosomes, were included at similar levels in the two exosome fractions (Fig. 1E). Although Hrs was not detected in the exosome fractions, TSG101 and VPS4B, two downstream ESCRT proteins, were clearly identified in the exosomes, and at lower amounts in the Hrs-depleted DCs. These data suggested that Hrs and another ESCRT trafficking pathway are involved in exosome secretion.

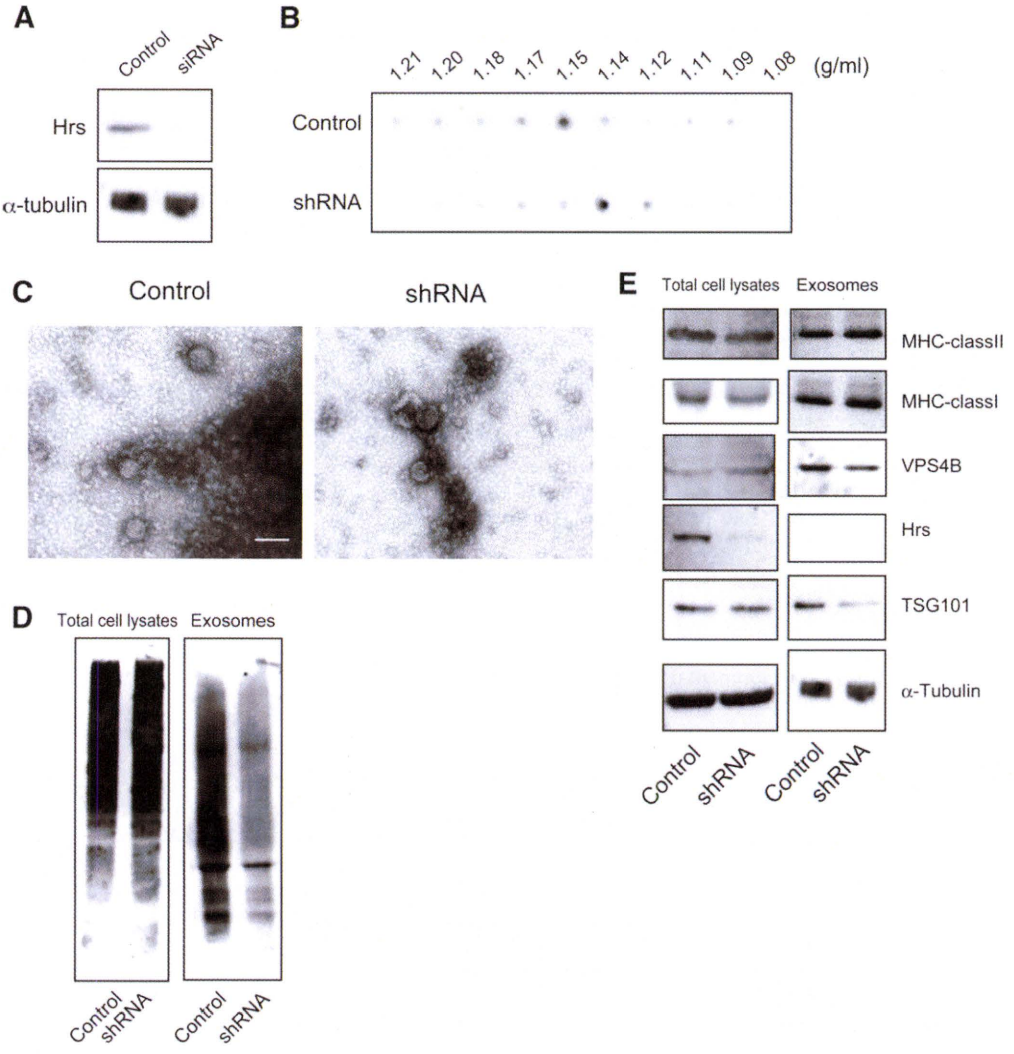

Fig. 1. Hrs-knock-down dendritic cells (DCs), Hrs knock-out bone marrow DCs, and characterization of their exosomes. (A) Western blot analysis of total cell lysates from control and Hrs knock-down DCs. (B) Sucrose gradient fractionation and dot-blot analysis of exosomes produced from DCs. The same amount of protein was fractionated and blotted on the membranes. (C) Negative staining TEM of exosomes from murine DCs. DCs were grown from monocytic precursors and cultured in GM-CSF for 10 days. The cell culture supernatants were sequentially centrifuged to obtain a pellet containing exosomes. The 100,000 x g pellet was washed and analyzed by TEM. Bar, 100 nm. (D) Western blot analysis of total cell lysates (left panel) and exosome fraction (right panel) using an antibody against ubiquitinated proteins (FK2). (E) Western blot analysis of total cell lysates (left panel) and exosomes (right panel) using the indicated antibodies.

3.2. Impairment of exosome secretion in Hrs-depleted DCs

In addition to steady-state secretion, DCs release additional exosomes upon stimulation. To examine the effect of Hrs on activation-dependent exosome secretion, the amount of purified exosomes released under several types of stimulation was measured. Ovalbumin (OVA) is known to induce exosome secretion from DCs [18,21]. Exosome secretion by the control DCs was clearly increased by 24 h of stimulation with OVA, whereas no significant increase was found in the Hrs-depleted DCs (Fig. 2A). To evaluate the possible effect of lipopolysaccharide (LPS) contamination in the OVA, we examined the amount of exosomes released under stimulation with LPS alone. Exosome secretion was not enhanced by the LPS stimulation, irrespective of the Hrs level (Fig. 2A). We also

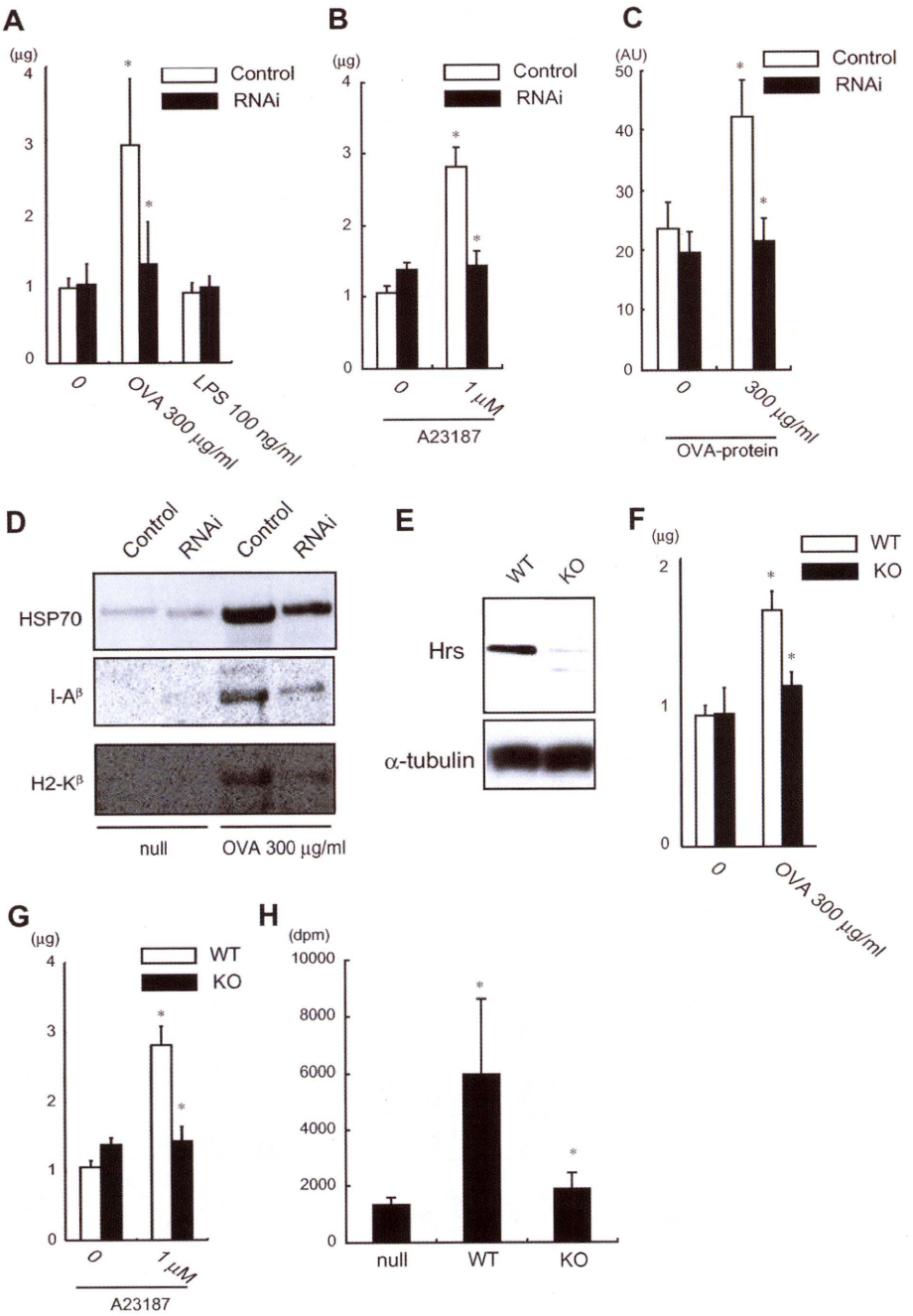

Fig. 2. Hrs is required for the secretion of exosomes. (A) Measurement of the exosome secretion from DCs under stimulation with OVA or LPS, using a protein assay. $^*p < 0.007$. (B) Measurement of exosomes under stimulation with a Ca^{2+} ionophore (1 μM A23187), using a protein assay. $^*p < 0.005$. (C) Measurement of exosome production under simulation with OVA, using N-Rh-PE release. $^*p < 0.05$. (D) Western blot analysis of exosomes under stimulation with OVA. (E) Western Blot analysis of total lysates from control and Hrs-knock out BMDCs. (F) Measurement of the exosome secretion from BMDCs under stimulation with OVA in BMDCs, using a protein assay. $^*p < 0.006$. WT, $hrs^{+/+}$, LysM-Cre; KO, $hrs^{flox/flox}$, LysM-Cre. (G) Measurement of exosomes under stimulation with a Ca^{2+} ionophore (1 μM A23187) in BMDCs, using a protein assay. $^*p < 0.005$. (H) [3H]-thymidine incorporation of CD8 T cells from OVA-specific TCR transgenic mice (OT-I mice). CD8 T cells were stimulated with purified exosomes from control and Hrs-knock out dendritic cells for 5 days. $^*p < 0.05$.

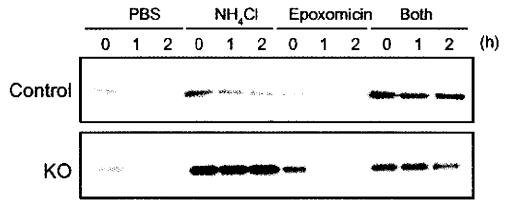

Fig. 3. Characteristics of Hrs-knock-out DCs under antigen stimulation. The degradation rate of OVA in control and Hrs-knock-down DCs was shown by western blot. A lysosomal inhibitor (NH_4Cl) and/or protease inhibitor (Epoxomicin) were included in the culture medium in some cases.

examined the exosome secretion induced by intracytoplasmic Ca^{2+} release [23]. The incubation of DCs with the Ca^{2+} ionophore A23187 induced a 2.8-fold increase in exosome release from the control DCs; however, the Hrs-depleted DCs showed very low Ca^{2+} responsiveness (Fig. 2B). We also measured the exosome secretion using N-(lissamine rhodamine B sulfonyl) phosphatidyl ethanolamine (N-Rh-PE) [10], and obtained similar results (Fig. 2C). Western blot analysis revealed that the levels of three exosome markers, HSP70, I-A^{β}, and H-2 K^{β}, were reduced in the Hrs-depleted DCs compared with the control DCs, after incubation with OVA (Fig. 2D).

To verify the essential role of Hrs in exosomal secretion, Hrs-depleted bone marrow-derived DCs (BMDCs) were successfully generated from $hrs^{flox/flox}$; LysM-Cre mice, and they expressed dramatically less Hrs than DCs derived from the $hrs^{+/+}$; LysM-Cre mice (Fig. 2E). No significant difference was seen between the population of $CD11c^{+}$ cells in BMDCs from $hrs^{+/+}$; LysM-Cre and $hrs^{flox/flox}$; LysM-Cre mice (data not shown). First, we examined the amount of exosome secretion under stimulation of OVA as well as Ca^{2+} ionophore A23187. Similar to the results obtained from Hrs-knock-down DCs, BMDCs from $hrs^{flox/flox}$; LysM-cre secreted lesser amount of exosome than those from $hrs^{+/+}$; LysM-Cre mice (Fig. 2F and G). We further investigated whether the Hrs depletion affected the amount of exosomes secreted from these cells, by measuring the antigen-presenting activity of the exosomes for T cells. DCs derived from the $hrs^{+/+}$; LysM-cre and $hrs^{flox/flox}$; LysM-Cre mice were incubated with OVA for 48 h, and the exosomes secreted from the DCs were purified. The exosomes were co-cultured with splenic $CD8^{+}$ T cells derived from OT-I transgenic mice. We found a significant increase in the proliferation of OVA-peptide restricted $CD8^{+}$ T cells cultured with the exosomes from the $hrs^{+/+}$; LysM-cre DCs, but not with those from the $hrs^{flox/flox}$; LysM-Cre DCs (Fig. 2H). Collectively, these data suggested that Hrs is required for exosome secretion.

3.3. No alteration in OVA degradation in Hrs-depleted DCs

It was possible that the decreased antigen-presentation activity of exosomes from the Hrs-depleted DCs was due to insufficient degradation of the OVA protein that was taken up. We therefore measured its degradation rate. The OVA protein was completely degraded one hour after the OVA pulse, and the degradation was the same, regardless of Hrs expression. The degradation of the OVA was efficiently blocked by a lysosomal acidification inhibitor, NH_4Cl, but not by a proteasomal inhibitor, epoxomicin, in both the control and the Hrs-depleted DCs (Fig. 3). These results suggested that Hrs does not affect the lysosome-dependent degradation of the OVA protein in DCs.

3.4. Characteristics of Hrs-depleted DCs under stimulation by OVA

We next investigated whether Hrs-depleted DCs were activated by stimulation with OVA. When stimulated with OVA proteins, DC activation markers increased more in Hrs-depleted DCs than in control cells (Fig. 4A to C). This was also true of the production of cytokines, including interleukin-6 (IL-6) and tumor necrosis factor-alpha (TNF-α) (Fig. 4D and E). These findings indicated that exosome secretion and DC activation were regulated by different mechanisms.

4. Discussion

There is accumulating evidence that the ESCRT proteins play important roles in the formation of MVBs, which undergo lysosomal digestion or are released into the extracellular environment as exosomes [24]. The ESCRT machinery, glycosylphosphatidylinositol-

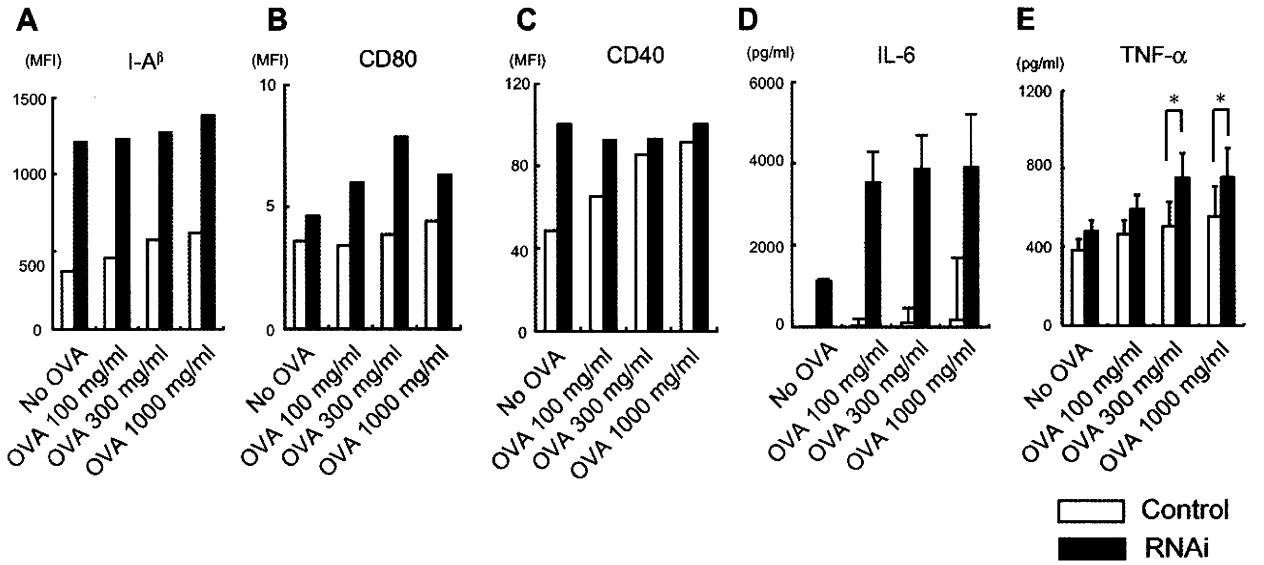

Fig. 4. Characteristics of Hrs-depleted DCs under stimulation of OVA (A to C) FACS analysis using anti-I-A^{β} (A), CD80 (B), and CD40 (C) antibodies. Control and Hrs-knock-down DCs were incubated with OVA for 24 h. Data are representative of at least three experiments. (D and E) Measurement of cytokine secretion from control and Hrs-knock-down DCs. Control and Hrs-knock-down DCs were incubated with OVA for 16 h. Data are representative of at least three experiments performed in triplicate. $^{*}p < 0.05$.

associated lipid affinity, and tetraspanin-associated protein affinity are involved in the mechanisms of cargo-protein sorting and intraluminal-vesicle formation, which are related to exosome maturation [25]. So far, two Ras family monomeric G protein Rab27a and Rab27b were reported to function in MVB docking at the plasma membrane, and to control the exosomal pathway [11], suggesting that MVBs contribute to exosome secretion through their direct fusion to the cell surface membranes. In this context, we demonstrated here that Hrs, one of the ESCRT proteins, is required for the production of exosomes within MVBs. Regarding the relationship between exosome production and the ESCRT machinery, there have been some contradictory reports. For example, the formation of proteolipid protein-containing exosomes is dependent on Rab5, but independent of the ESCRT machinery in oligodendrocytes under ceramide stimulation [12]. Since our present study on exosome production was limited to DCs stimulated by OVA or a calcium ionophore, there may be some cargo-dependent or stimulation-dependent pathways for MVB formation and exosome production.

In antigen-presenting cells, exosomes are secreted upon exposure to various stimulants, such as OVA or the calcium ionophore A23187 [18]. OVA is usually considered to act as an antigenic peptide source, and other report also utilized this agent alone to stimulate DCs [26], although we cannot fully exclude a possibility that a faint contamination of LPS as a stimulator is included in OVA. The exosome secretion in Hrs-depleted DCs was decreased in spite of their higher expression of the cell-surface-activation markers, MHC class I/II molecules as compared with the control DCs. Those markers are also known to be ubiquitinated and sequestered through MVBs [27,28]. Therefore, our findings suggested that Hrs is required for the efficient endocytosis and degradation of the MHC molecules through MVB formation as well as the exosome secretion. We previously demonstrated that the deficiency of Hrs suppresses degradation of gp130, a subunit of IL-6 receptor, in HeLa cells, which leads to a prolonged and amplified IL-6 signal [8]. Epidermal growth factor receptor (EGFR) degradation is impaired and the signaling is enhanced in Hrs-depleted mouse embryonic fibroblasts and *Drosophila* [29,30]. We suspect that Hrs-depleted DCs may be more sensitive to some stimulations than control DCs. This may be true of IL-6 secretion, because the Hrs-depleted cells secreted small but significantly more IL-6 even in the absence of OVA (Fig. 4D). It is possible that IL-6 secretion is somewhat enhanced by a factor(s) contained in FCS in the medium without OVA stimulation. We suspect that both the prolongation of cytokine signals and the deficiency of exosome production in Hrs-depleted DCs are caused by the impaired MVB formation.

Finally, our present study suggests a biological role of Hrs in immune regulation (Fig. 2H). DC-derived exosomes have been shown to have potent immunostimulatory potential, and MHC-I and B7.2 (CD86)-bearing exosomes generate $CD8^+$ T-cell responses against tumors in vivo [31]. Further study using DC-specific Hrs knockout mice will provide precise roles of the Hrs-dependent exosomal pathway in anti-tumor immune response.

Acknowledgments

The LysM-cre transgenic mice were kindly provided by Dr. Irmgard Foerster (Technical University of Munich, Munich, Germany). The authors thank Ms. Rie Ito and Yoshihiko Fujioka for technical assistance. This work was supported by JSPS and MEXT KAKENHI (21590517, 19059001, and 22790630) and a Grant-in-Aid from Ministry of Health, Labour and Welfare.

References

[1] B. Fevrier, G. Raposo, Exosomes: endosomal-derived vesicles shipping extracellular messages, Curr. Opin. Cell. Biol. 16 (2004) 415–421.
[2] G. Raposo, H.W. Nijman, W. Stoorvogel, R. Liejendekker, C.V. Harding, C.J. Melief, H.J. Geuze, B lymphocytes secrete antigen-presenting vesicles, J. Exp. Med. 183 (1996) 1161–1172.
[3] M. Karlsson, S. Lundin, U. Dahlgren, H. Kahu, I. Pettersson, E. Telemo, "Tolerosomes" are produced by intestinal epithelial cells, Eur. J. Immunol. 31 (2001) 2892–2900.
[4] S. Ostman, M. Taube, E. Telemo, Tolerosome-induced oral tolerance is MHC dependent, Immunology 116 (2005) 464–476.
[5] S.I. Buschow, J.M. Liefhebber, R. Wubbolts, W. Stoorvogel, Exosomes contain ubiquitinated proteins, Blood Cells Mol. Dis. 35 (2005) 398–403.
[6] H. Asao, Y. Sasaki, T. Arita, N. Tanaka, K. Endo, H. Kasai, T. Takeshita, Y. Endo, T. Fujita, K. Sugamura, Hrs is associated with STAM, a signal-transducing adaptor molecule. Its suppressive effect on cytokine-induced cell growth, J. Biol. Chem. 272 (1997) 32785–32791.
[7] M. Komada, N. Kitamura, Growth factor-induced tyrosine phosphorylation of Hrs, a novel 115-kilodalton protein with a structurally conserved putative zinc finger domain, Mol. Cell. Biol. 15 (1995) 6213–6221.
[8] Y. Tanaka, N. Tanaka, Y. Saeki, K. Tanaka, M. Murakami, T. Hirano, N. Ishii, K. Sugamura, c-Cbl-dependent monoubiquitination and lysosomal degradation of gp130, Mol. Cell Biol. 28 (2008) 4805–4818.
[9] S.I. Buschow, E.N. Nolte-'t Hoen, G. van Niel, M.S. Pols, T. ten Broeke, M. Lauwen, F. Ossendorp, C.J. Melief, G. Raposo, R. Wubbolts, M.H. Wauben, W. Stoorvogel, MHC II in dendritic cells is targeted to lysosomes or T cell-induced exosomes via distinct multivesicular body pathways, Traffic 10 (2009) 1528–1542.
[10] A. Savina, M. Vidal, M.I. Colombo, The exosome pathway in K562 cells is regulated by Rab11, J. Cell Sci. 115 (2002) 2505–2515.
[11] M. Ostrowski, N.B. Carmo, S. Krumeich, I. Fanget, G. Raposo, A. Savina, C.F. Moita, K. Schauer, A.N. Hume, R.P. Freitas, B. Goud, P. Benaroch, N. Hacohen, M. Fukuda, C. Desnos, M.C. Seabra, F. Darchen, S. Amigorena, L.F. Moita, C. Thery, Rab27a and Rab27b control different steps of the exosome secretion pathway, Nat. Cell Biol. 12 (2010) 19–30. sup pp 11-13.
[12] K. Trajkovic, C. Hsu, S. Chiantia, L. Rajendran, D. Wenzel, F. Wieland, P. Schwille, B. Brugger, M. Simons, Ceramide triggers budding of exosome vesicles into multivesicular endosomes, Science 319 (2008) 1244–1247.
[13] M.B. Lutz, N. Kukutsch, A.L. Ogilvie, S. Rossner, F. Koch, N. Romani, G. Schuler, An advanced culture method for generating large quantities of highly pure dendritic cells from mouse bone marrow, J. Immunol. Methods 223 (1999) 77–92.
[14] K. Tamai, N. Tanaka, A. Nara, A. Yamamoto, I. Nakagawa, T. Yoshimori, Y. Ueno, T. Shimosegawa, K. Sugamura, Role of Hrs in maturation of autophagosomes in mammalian cells, Biochem. Biophys. Res. Commun. 360 (2007) 721–727.
[15] K. Tamai, M. Toyoshima, N. Tanaka, N. Yamamoto, Y. Owada, H. Kiyonari, K. Murata, Y. Ueno, M. Ono, T. Shimosegawa, N. Yaegashi, M. Watanabe, K. Sugamura, Loss of hrs in the central nervous system causes accumulation of ubiquitinated proteins and neurodegeneration, Am. J. Pathol. 173 (2008) 1806–1817.
[16] B.E. Clausen, C. Burkhardt, W. Reith, R. Renkawitz, I. Forster, Conditional gene targeting in macrophages and granulocytes using LysMcre mice, Transgenic Res. 8 (1999) 265–277.
[17] S.R. Clarke, M. Barnden, C. Kurts, F.R. Carbone, J.F. Miller, W.R. Heath, Characterization of the ovalbumin-specific TCR transgenic line OT-I: MHC elements for positive and negative selection, Immunol. Cell. Biol. 78 (2000) 110–117.
[18] S. Hao, O. Bai, J. Yuan, M. Qureshi, J. Xiang, Dendritic cell-derived exosomes stimulate stronger $CD8^+$ CTL responses and antitumor immunity than tumor cell-derived exosomes, Cell. Mol. Immunol. 3 (2006) 205–211.
[19] J. Willem, M. ter Beest, G. Scherphof, D. Hoekstra, A non-exchangeable fluorescent phospholipid analog as a membrane traffic marker of the endocytic pathway, Eur. J. Cell. Biol. 53 (1990) 173–184.
[20] N. Tanaka, K. Kaneko, H. Asao, H. Kasai, Y. Endo, T. Fujita, T. Takeshita, K. Sugamura, Possible involvement of a novel STAM-associated molecule "AMSH" in intracellular signal transduction mediated by cytokines, J. Biol. Chem. 274 (1999) 19129–19135.
[21] S. Hao, O. Bai, F. Li, J. Yuan, S. Laferte, J. Xiang, Mature dendritic cells pulsed with exosomes stimulate efficient cytotoxic T-lymphocyte responses and antitumour immunity, Immunology 120 (2007) 90–102.
[22] C. Thery, A. Regnault, J. Garin, J. Wolfers, L. Zitvogel, P. Ricciardi-Castagnoli, G. Raposo, S. Amigorena, Molecular characterization of dendritic cell-derived exosomes. Selective accumulation of the heat shock protein hsc73, J. Cell Biol. 147 (1999) 599–610.
[23] A. Savina, C.M. Fader, M.T. Damiani, M.I. Colombo, Rab11 promotes docking and fusion of multivesicular bodies in a calcium-dependent manner, Traffic 6 (2005) 131–143.
[24] A. de Gassart, C. Geminard, D. Hoekstra, M. Vidal, Exosome secretion: the art of reutilizing nonrecycled proteins?, Traffic 5 (2004) 896–903
[25] G. van Niel, I. Porto-Carreiro, S. Simoes, G. Raposo, Exosomes: a common pathway for a specialized function, J. Biochem. 140 (2006) 13–21.
[26] K. Akiyama, S. Ebihara, A. Yada, K. Matsumura, S. Aiba, T. Nukiwa, T. Takai, Targeting apoptotic tumor cells to Fc gamma R provides efficient and versatile vaccination against tumors by dendritic cells, J. Immunol. 170 (2003) 1641–1648.

[27] L.M. Duncan, S. Piper, R.B. Dodd, M.K. Saville, C.M. Sanderson, J.P. Luzio, P.J. Lehner, Lysine-63-linked ubiquitination is required for endolysosomal degradation of class I molecules, EMBO. J. 25 (2006) 1635–1645.
[28] J.S. Shin, M. Ebersold, M. Pypaert, L. Delamarre, A. Hartley, I. Mellman, Surface expression of MHC class II in dendritic cells is controlled by regulated ubiquitination, Nature 444 (2006) 115–118.
[29] T.E. Lloyd, R. Atkinson, M.N. Wu, Y. Zhou, G. Pennetta, H.J. Bellen, Hrs regulates endosome membrane invagination and tyrosine kinase receptor signaling in Drosophila, Cell 108 (2002) 261–269.
[30] C. Kanazawa, E. Morita, M. Yamada, N. Ishii, S. Miura, H. Asao, T. Yoshimori, K. Sugamura, Effects of deficiencies of STAMs and Hrs, mammalian class E Vps proteins, on receptor downregulation, Biochem. Biophys. Res. Commun. 309 (2003) 848–856.
[31] L. Zitvogel, A. Regnault, A. Lozier, J. Wolfers, C. Flament, D. Tenza, P. Ricciardi-Castagnoli, G. Raposo, S. Amigorena, Eradication of established murine tumors using a novel cell-free vaccine: dendritic cell-derived exosomes, Nat. Med. 4 (1998) 594–600.

Research Article

EASL EUROPEAN ASSOCIATION FOR THE STUDY OF THE LIVER | JOURNAL OF HEPATOLOGY

Possible involvement and the mechanisms of excess *trans*-fatty acid consumption in severe NAFLD in mice

Noriyuki Obara[1], Koji Fukushima[1], Yoshiyuki Ueno[1,*], Yuta Wakui[1], Osamu Kimura[1], Keiichi Tamai[1], Eiji Kakazu[1], Jun Inoue[1], Yasuteru Kondo[1], Norihiko Ogawa[2], Kenta Sato[3], Tsuyoshi Tsuduki[3], Kazuyuki Ishida[4], Tooru Shimosegawa[1]

[1]*Division of Gastroenterology, Tohoku University Graduate School of Medicine, 1-1 Seiryo, Aobaku, Sendai 980-8574, Japan;* [2]*Division of Advanced Surgical Science and Technology, Graduate School of Medicine, Tohoku University, Sendai, Japan;* [3]*Laboratory of Food and Biomolecular Science, Graduate School of Agricultural Science, Tohoku University, Sendai, Japan;* [4]*Department of Pathology, Tohoku University Hospital, Sendai, Japan*

Background & Aims: Excessive *trans*-fatty acids (TFA) consumption has been thought to be a risk factor mainly for coronary artery diseases while less attention has been paid to liver disease. We aimed to clarify the impact of TFA-rich oil consumption on the hepatic pathophysiology compared to natural oil.

Methods: Mice were fed either a low-fat (LF) or high-fat (HF) diet made of either natural oil as control (LF-C or HF-C) or partially hydrogenated oil, TFA-rich oil (LF-T or HF-T) for 24 weeks. We evaluated the liver and body weight, serological features, liver lipid content and composition, liver histology and hepatic lipid metabolism-related gene expression profile. In addition, primary cultures of mice Kupffer cells (KCs) were evaluated for cytokine secretion and phagocytotic ability after incubation in *cis*- or *trans*-fatty acid-containing medium.

Results: The HF-T-fed mice showed significant increases of the liver and body weights, plasma alanine-aminotransferase, free fatty acid and hepatic triglyceride content compared to the HF-C group, whereas the LF-T group did not differ from the LF-C group. HF-T-fed mice developed severe steatosis, along with increased lipogenic gene expression and hepatic TFA accumulation. KCs showed increased tumor necrosis factor secretion and attenuated phagocytotic ability in the TFA-containing medium compared to its *cis*-isomer.

Conclusions: Excessive consumption of the TFA-rich oil up-regulated the lipogenic gene expression along with marked hepatic lipid accumulation. TFA might be pathogenic through causing severe steatosis and modulating the function of KCs. The quantity and composition of dietary lipids could be responsible for the pathogenesis of non-alcoholic steatohepatitis.

Keywords: *trans*-Fatty acid; NASH; NAFLD; Metabolic syndrome; Kupffer cell.
Received 16 September 2009; received in revised form 18 January 2010; accepted 26 February 2010

*Corresponding author. Tel.: +81 22 717 7171; fax: +81 22 717 7177.
E-mail address: yueno@mail.tains.tohoku.ac.jp (Y. Ueno).

Abbreviations: NAFLD, non-alcoholic fatty liver disease; NASH, non-alcoholic steatohepatitis; FFA, free fatty acid; LPS, lipopolysaccharide; TFA, *trans*-fatty acid; ALT, alanine-aminotransferase; LF(-C or -T), low-fat (control or TFA-rich) diet; HF(-C or -T), high-fat (control or TFA-rich) diet; KCs, Kupffer cells (KCs); AST, aspartate-aminotransferase; TG, triglyceride; ELISA, Enzyme-Linked ImmunoSorbent Assay; HDL, high density lipoprotein; (V)LDL, (very) low density lipoprotein; NAS, NAFLD activity score; TBARS, thiobarbituric acid reactive substances; TNFα, tumor necrosis factor α; IL-6, interleukin-6; SD, standard deviation; iNOS, inducible nitric oxide synthase; TGF-β, transforming growth factor-β; SREBP-1, sterol regulatory element-binding protein-1; FAS, fatty acid synthase; ACC, acetyl CoA carboxylase; PPAR, peroxisome proliferator activated receptor; PGC-1β, PPARγ coactivator-1β; PUFA, polyunsaturated fatty acid; MUFA, monounsaturated fatty acid; SFA, saturated fatty acid.

Introduction

In concordance with the prevalence of obesity, the incidence of non-alcoholic fatty liver disease (NAFLD) has increased and is nowadays recognized as the most common liver disease [2]. It is known that a part of NAFLD can progress to non-alcoholic steatohepatitis (NASH), liver fibrosis, cirrhosis and hepatocellular carcinoma [9]. Nevertheless, the mechanisms of NAFLD-to-NASH transition remain to be clarified; NAFLD appears to originate from the dysregulation of hepatic lipid metabolism as a part of the metabolic syndrome accompanied by visceral obesity, dyslipidemia, atherosclerosis, and insulin resistance [25]. According to the hypothetical theory named the 2-hit theory [5], the secondary hit to NAFLD that can be due to free fatty acid (FFA)s, oxidative stress, lipopolysaccharide (LPS) and inflammatory cytokines, causes NASH as a consequence.

In terms of the "first hit", the lipid accumulation in the liver is induced by high-fat diets [6,23] that include various lipid species. Such dietary lipid species uniquely affect the obesity phenotype, liver histology and gene expression pattern in the rat liver [3]. In this context, lipid species could play a potential role in the pathogenesis of NAFLD and/or NASH.

trans-Fatty acid (TFA) is produced through the industrial hardening of the vegetable oils to make the products more stable and robust, and thus easier to handle or store. Excess consumption of TFA is known as a risk factor for coronary artery diseases, insulin resistance and obesity accompanied by systemic inflammation, the features of metabolic syndrome [20,29]. Nevertheless, little is known about the effects on the liver induced by lipids.

Please cite this article in press as: Obara N et al. Possible involvement and the mechanisms of excess *trans*-fatty acid consumption in severe NAFLD in mice. J Hepatol (2010), doi:10.1016/j.jhep.2010.02.029

Research Article

Fast-foods, containing large amount of TFA in the form of margarine, spreads or frying oils, cause body-weight gain and abnormal serum alanine-aminotransferase (ALT) elevations in healthy subjects [15]. In addition, TFA-rich chow leads to hepatic steatosis [30], ALT elevations and insulin resistance in mice [17]; although the mechanisms have not been completely clarified. Therefore, we aimed to investigate the impact of the dietary lipid species and their quantities on the pathogenicity of hepatic inflammation and steatosis in mice. Comparing in particular natural oil and industrially produced partially hydrogenated TFA-rich oil of the same origin.

Materials and methods

Animal treatment

All the animal experiments were conducted under the approval of the Institutional Animal Care and Use Committees of Tohoku University. Female C57BL/6Njcl mice (8–10 weeks) were randomly assigned to four groups ($n = 6$ per group) and fed the designated chows (ORIENTAL YEAST Co. Ltd., Tokyo, Japan) *ad libitum* for 24 weeks, respectively. Low-fat diet (LF) and high-fat diet (HF) were made of either natural canola oil as control oil (LF-C and HF-C) or industry produced partially hydrogenated canola oil as TFA-rich oil (28.5% TFA/total fat, LF-T and HF-T), respectively (Table 1). After 12 h of fasting, the mice were sacrificed under diethylether anesthesia and the livers were removed and weighed. The divided livers were either stored at −80 °C for lipid, protein and gene expression analysis, or fixed in 4% paraformaldehyde and embedded in paraffin for histological evaluation. Standard chow-fed female C57BL/6Njcl mice (6–10 weeks) were used as a source of primary Kupffer cells (KCs).

Chemistry

Plasma aspartate-aminotransferase (AST), ALT, triglyceride (TG) and total cholesterol were measured with FUJI DRI-CHEM 7000 (FUJIFILM, Tokyo, Japan) at Biomedical Research Core of Tohoku University Graduate School of Medicine. Plasma adiponectin (AdipoGen, Seoul, Korea) and leptin (RayBio, GA, USA) were measured by Enzyme-Linked ImmunoSorbent Assay (ELISA). Plasma FFA, high density lipoprotein (HDL)-cholesterol and (very) low density lipoprotein ((V)LDL)-cholesterol were measured by enzymatic assay kits (BioVision, CA, USA).

Histology and immunohistochemistry

The thin-sliced specimens were stained with hematoxylin and eosin to evaluate steatosis and inflammation or Sirius red to evaluate fibrosis of the liver. The histology was scored by the NAFLD activity score (NAS) [16]. KCs were stained with anti-F4/80 monoclonal antibody (Abcam, Cambridge, UK) and neutrophils were detected by myeroperoxidase immunostaining (Abcam). Apoptosis was evaluated by TUNEL method using an ApopTag kit (Chemicon, CA, USA).

Table 1. Diet compositions.

	Low-fat diet		High-fat diet	
	Control oil (LF-C) kcal%	TEA-rich oil (LF-T) kcal%	Control (HF-C) kcal%	TEA-rich (HF-T) kcal%
Diet compositions				
Protein	13.8	13.8	18.8	18.8
Carbohydrate	74.4	74.4	17.6	17.6
Over all fat	11.8	11.8	63.6	63.6
Fat composition (g/100 g)				
Saturated	7.8	21.7	7.8	21.7
(*cis*-)Monounsaturated	62.5	45.3	62.5	45.3
Polyunsaturated	29.7	4.5	29.7	4.5
trans- (%)		28.5		28.5

Immunoblot analysis and real-time RT-PCR

Liver protein extracts were evaluated by immunoblot analysis with the following primary antibodies: phosphor-AKT (Thr308 and Ser473), total AKT (Cell Signaling Technology, Danvers, MA) and β-actin (Sigma, MO, USA). RNA extracted from the livers was subjected to real-time RT-PCR analysis using the specifically designed primer sets purchased form TAKARA BIO Perfect Real Time Support System (TAKARA BIO INC., Tokyo, Japan) and One Step SYBR Prime Script RT-PCR Kit II (TAKARA BIO INC.), and only PGC-1β was analyzed using the specifically designed TaqMan primer set and 1-step kit (Applied Biosystems, CA, USA). All results were normalized by GAPDH as the internal control.

Lipidomic analysis of the liver

Hepatic TG and FFA content were measured by enzymatic assay kit (BioVision) and were normalized by the liver weight. Hepatic lipid peroxide was evaluated by measuring TBARS (thiobarbituric acid reactive substances, Cayman Chemical Company, USA) in the liver and was normalized by the protein level [18]. Total lipids from the liver were extracted by Folch's procedure [10]. The lipids were methylated and evaluated by gas chromatography as previously reported [31].

Isolation and culture of primary Kupffer cells

KCs were isolated as reported previously [28]. Briefly, the mice livers were digested by two-step collagenase perfusion. The minced livers were subjected to the gradient centrifugation of Percoll (Sigma) and succeeding counterflow centrifugal elutriation. The viabilities of the obtained cells evaluated by trypan blue staining were more than 85%, and the purity was more than 90% determined by the population of CD11b positive cells counted by FACS Calibur (Becton Dickinson, Tokyo, Japan). KCs were suspended in RPMI1640 medium with 10% fetal bovine serum and antibiotics (100 U/ml penicillin G, 100 μg/ml streptomycin sulfate) and incubated overnight at 37 °C in 5% CO_2 incubator for the succeeding examinations.

Fatty acid treatment

Fatty acids (Larodan Fine Chemicals, Malmo, Sweden) were dissolved in RPMI1640 medium with 1% fatty acid-free bovine serum albumin (Calbiochem, Darmstadt, Germany) and adjusted to a final concentration of 200 μM with 1% bovine serum albumin, 1% ITS-A supplement (GIBCO, CA, USA) and antibiotics same as above. After overnight incubation, KCs were washed and the medium was changed to fatty acid-containing medium or fatty acid-free medium as the control, and incubated for another 24 h.

Cytokine production by KCs stimulated with lipopolysaccharide

After 24 h incubation, KCs were stimulated by LPS (100 ng/ml, SIGMA) combined with LPS-binding protein (200 pg/ml, ALEXIS BIOCHEMICALS, Lausanne, Switzerland) for 6 h, and the cell viability was determined by MTS assay (3-(4,5-dimethylthiazol-2-yl)-5-(3-carboxymethoxyphenyl)-2-(4-sulfophenyl)-2*H*-tetrazolium, inner salt and phenazine ethosulfate, Promega, Tokyo, Japan). The supernatants were subjected to ELISA (Thermo Fisher Scientific Inc., IL, USA) for the evaluation of the tumor necrosis factor-alfa (TNFα) and interleukin-6 (IL-6) production.

Phagocytotic ability of KCs

After 24 h incubation, KCs were incubated at 37 °C for 1 h with 1 μm latex beads (75 ng/ml, SIGMA) or at 4 °C in the fatty acid-free medium as control. After incubation, the cells were washed 3 times, detached with trypsin/EDTA and analyzed by FACS calibur [1].

Statistical analysis

The results are shown as the mean ± standard deviation (SD), and were analyzed by SPSS software (SPSS INC., Tokyo, Japan).

The differences between the groups were tested by ANOVA, followed by Tukey post hoc test. A p values less than 0.05 were considered statistically significant.

Please cite this article in press as: Obara N et al. Possible involvement and the mechanisms of excess *trans*-fatty acid consumption in severe NAFLD in mice. J Hepatol (2010), doi:10.1016/j.jhep.2010.02.029

Results

Physiological and biochemical characteristics

Body weight was similar between LF-fed mice, increased in HF-fed mice compared to LF-fed mice, and strikingly HF-T-fed mice weighed 1.3-fold more than HF-C-fed mice (Table 2). Liver weight was significantly increased in only HF-T-fed mice by approximately 2-fold compared to the other groups. The liver–body weight ratio was significantly increased by 1.2- and 1.6-fold in LF-T-fed and HF-T-fed mice, respectively, compared to the corresponding control groups with the same dietary composition, and decreased by approximately 20% in the HF-C-fed mice compared to the LF-C-fed mice.

Plasma AST, ALT, TG, FFA and leptin were similar between the LF groups irrespective of the dietary lipid source, but in the LF-T group, total cholesterol, HDL-cholesterol, (V)LDL-cholesterol and adiponectin were significantly decreased compared to the LF-C group (Table 2). In contrast, some serum markers were elevated in the HF-T group compared to the HF-C group, particularly AST, ALT, TG, total cholesterol, (V)LDL-cholesterol, FFA and leptin were significantly increased. As for the control oil-fed mice, total cholesterol, HDL-cholesterol, (V)LDL-cholesterol and adiponectin were lower, whereas plasma leptin was higher in HF-C-fed than in LF-C-fed mice. Between TFA-rich oil-fed mice, all serum markers except adiponectin were also significantly higher in HF-T-fed than in LF-T-fed mice.

Liver histology

There were few lipid droplets in LF-C-fed mice liver. Mild microvesicular and macrovesicular steatosis was present around zone 1 in LF-T-fed mice livers and abundant large lipid droplets around zones 1 and 2 in HF-C-fed mice livers. Inflammation and ballooning degeneration were minimal in these groups (Fig. 1A). However, the HF-T-fed mice livers were characterized by foamy, prominent microvesicular steatosis throughout the lobe and some macrovesicular lipid droplets in zones 1 and 2. Most of the hepatocytes were expanded with marked small lipid droplets that surrounded the nuclei, and the severely expanded hepatocytes presented the phenotype of ballooning degeneration (Fig. 1A); moreover, some of the fatty hepatocytes were surrounded by infiltrated neutrophils confirmed by immunostaining for myeloperoxidase, forming lipogranuloma (Fig. 1B) accompanied by ballooning hepatocytes (Fig. 1C). The number of neutrophils was increased in HF-T-fed mice livers (Fig. 1D). However, when evaluated by NAS, the HF-T group did not show significant differences (Table 2).

To investigate the involvement of KCs in the pathological difference between the HF-C group and HF-T group, we performed immunohistochemical staining for F4/80, a macrophage-restricted surface glycoprotein. F4/80-positive cells were more prevalent in the HF-T group (Fig. 1E). Although fibrosis was not identified visually by Sirius red staining in any of the groups (not shown), collagen type1, α1 mRNA expression in the liver, as an early fibrosis marker, increased only in HF-T-fed mice by 3.6-fold compared to LF-C-fed mice (Fig. 1F). TUNEL assay did not reveal conspicuous apoptotic hepatocytes in each group, however some non-parenchymal cells were TUNEL positive (Supplementary Fig. 1).

Lipid and lipid peroxide content and fatty acid composition of liver

The hepatic total lipid (Fig. 2A), TG (Fig. 2B), FFA (Fig. 2C) and lipid peroxide contents (Fig. 2D) did not differ between the LF-C and LF-T groups. On the other hand, reflecting the marked liver weight gain and histological steatotic changes, hepatic total lipid, TG and lipid peroxide content were significantly increased in the HF-T group compared to the HF-C group, while FFA content did not differ. All of these markers had a tendency to be elevated in the HF groups compared to the LF groups and when compared between the corresponding dietary oil-fed groups, although the TG increase in HF-C-fed mice was not statistically significant.

Table 2. Influence of *trans*-fatty acid-rich oil intake for the physiological and biochemical characteristics.

	Low-fat diet		High-fat diet	
	Control oil (LF-C)	TFA-rich oil (LF-T)	Control oil (HF-C)	TFA-rich oil (HF-T)
Body weight (g)	24.4 ± 2.1	23.1 ± 1.3	31.8 ± 3.6‡	40.9 ± 7.0*‡†
Liver weight (g)	1.08 ± 0.16	1.22 ± 0.08	1.11 ± 0.11	2.40 ± 1.01*‡†
Liver–body weight ratio (%)	4.5 ± 0.4	5.4 ± 0.2*	3.5 ± 0.3‡	5.6 ± 1.6*†
Plasma characteristics				
Aspartate-aminotransferase (IU/L)	95.2 ± 12.4	82.5 ± 20.8	136.8 ± 47.0	262.2 ± 72.0*‡†
Alanine-aminotransferase (IU/L)	48.8 ± 15.0	37.0 ± 7.3	50.4 ± 10.9	244.0 ± 105.7*‡†
Triglyceride (mg/dl)	60.3 ± 19.2	51.0 ± 12.8	62.4 ± 14.8	124.8 ± 45.0*‡†
Total cholesterol (mg/dl)	77.0 ± 8.9	47.5 ± 6.1*	55.2 ± 5.0	87.8 ± 10.1*‡
HDL-cholesterol (mg/dl)	51.6 ± 8.3	26.2 ± 3.9*	33.3 ± 7.2‡	38.6 ± 5.0‡†
(V)LDL-cholesterol (mg/dl)	16.8 ± 2.1	12.0 ± 1.5*	11.9 ± 1.0‡	17.4 ± 1.7*‡
Free fatty acids (nmol/ml)	1.77 ± 0.38	1.43 ± 0.31	1.99 ± 0.58	3.64 ± 0.42*‡†
Adiponectin (μg/ml)	25.5 ± 1.4	18.2 ± 1.4*	20.0 ± 1.5‡	20.0 ± 1.4†
Leptin (ng/L)	5.6 ± 0.7	5.3 ± 0.6	13.8 ± 2.0‡	23.7 ± 2.3*‡†
Total: HDL-cholesterol ratio	1.54 ± 0.06	2.33 ± 0.5*	1.71 ± 0.37	2.25 ± 0.87†
NAFLD activity score				
Steatosis	0.33 ± 0.52	0.17 ± 0.41	1.67 ± 0.82‡	1.17 ± 0.41‡
Inflammation	0.33 ± 0.52	0.33 ± 0.52	0.83 ± 0.75	1.00 ± 0.63
Ballooning	0.00 ± 0.00	1.00 ± 0.63*	1.00 ± 0.00‡	1.67 ± 0.82†

All values are means ± SD (n = 6 per each group).

* Significantly different from the corresponding control group with the same dietary composition; $p < 0.05$.

‡ Significantly different from the low-fat diet with the same dietary lipid as a source; $p < 0.05$.

† Significantly different from low-fat control diet group; $p < 0.05$.

Please cite this article in press as: Obara N et al. Possible involvement and the mechanisms of excess *trans*-fatty acid consumption in severe NAFLD in mice. J Hepatol (2010), doi:10.1016/j.jhep.2010.02.029